AIMS Mathematics

https://www.aimspress.com/journal/Math

AIMS Mathematics, 11(7): 20473–20501.
DOI:10.3934/math.2026833
Received: 11 April 2026
Revised: 16 June 2026
Accepted: 29 June 2026
Published: 13 July 2026

Research article

Event-triggered fixed-time consensus tracking of nonlinear delayed multi-agent systems with disturbances under switching topologies

Mingqiang Meng[1], Kaiquan Xiang[1], Qintao Gan[1] and Lei Chang[2,*]

[1] Shijiazhuang Campus, Army Engineering University of PLA, Shijiazhuang 050003, China
[2] Weapons and Control Department, Army Academy of Armored Forces, Beijing 100072, China

* **Correspondence:** Email: changleinew@163.com.

Abstract: This work investigated the fixed-time consensus (FxTC) tracking problem for nonlinear multi-agent systems (MASs), considering input delay and external disturbances, via an event-triggered (ET) mechanism under undirected fixed and switching topologies. To begin with, a novel ET controller was designed. Its distinctive feature is the inclusion of the constant delay term and compensation terms, which is different from the existing protocols. Consequently, it provides designers with flexible options for practical implementations in the context of time-delay systems subject to external disturbances. Through this approach, under fixed topology, all follower agents were able to achieve FxTC tracking, and importantly, a settling time (ST) upper bound was directly computed by using the system's predetermined parameters. Furthermore, it was rigorously proven that Zeno behavior was excluded. Then, those results were extended to switching topologies. The presented controller guarantees FxTC while significantly reducing both its update frequency and the overall energy consumption of the system. Finally, simulation examples were carried out to demonstrate the validity of proposed findings.

Keywords: multi-agent systems; event-triggered; fixed-time consensus; external disturbance; switching topologies
Mathematics Subject Classification: 91D30, 93A16, 93D50

1. Introduction

During the last few years, MASs have garnered significant attention from the academic community owing to their wide range of applications in some disciplines, for instance, unmanned aerial vehicle (UAV) formation [1], intelligent traffic control [2], robots [3], and many others. The consensus, as one of the core issues in MAS research, aims to design control protocols to make the states of all agents ultimately reach a common value. For example, in UAV platooning [1], consensus protocols ensure that the fleet maintains a preset formation and speed; in power systems [4], they enable power-sharing among distributed generation units.

Recently, a substantial amount of research has been devoted to addressing the consensus of MASs. For example, finite-time consensus has been extensively studied in [5–7], which ensures that system states converge within a finite time and offer better robustness. However, a well-known limitation is that the ST generally relies on the system's initial conditions, which is difficult to estimate a priori in practical scenarios. To further address this issue, FxTC was proposed, where the ST upper bound is an initial-condition-independent constant and can be predetermined by control parameters, thereby attracting the attention of numerous scholars, who have begun to investigate FxTC in MASs [8–10]. Given the significant advantages of it in terms of convergence speed and predictability, it motivates us to study the FxTC tracking problem of MASs.

In practical MASs, time delays in information transmission are ubiquitous. Factors such as bandwidth limitations in communication networks, signal transmission distances, and data packet congestion inevitably introduce time delays. However, communication delays between neighboring agents can severely impact system performance and, in extreme cases, cause system instability. Therefore, studying the consensus problem of delayed MASs holds significant theoretical and practical importance. Recently, notable research results have been found for the consensus issue considering communication delays. For example, the time-varying control method was used to study the consensus of MASs under delayed communications in [11], and the model predictive control and leader-following consensus of MASs with communication delays were investigated in [12, 13], respectively. However, many studies on FxTC for delayed systems, such as [14–16], are predominantly based on fixed topologies. Nevertheless, due to factors like communication link interruptions, addition or removal of nodes, and the dynamic changes of mobile network topologies, communication topologies are often time-varying. Therefore, studying consensus under switching topologies is more challenging and general. Some literature has begun to focus on this direction. For instance, practical fixed-time output feedback containment control for MASs was investigated under switching topologies [17], the fixed-time average consensus problem for time-delay MASs was explored in the presence of switching topologies [18], and the prescribed-time consensus of MASs was studied under switching topologies [19]. These studies have advanced the development of consensus theory in dynamic network environments. It is worth mentioning that few works have focused on the problem of FxTC tracking for delayed MASs under switching topologies. Inspired by the above analysis, it is feasible to address FxTC tracking of the delayed MASs under switching topologies.

In addition, to ensure system convergence performance, control cost is also a critical factor in controller design. Many of the aforementioned studies, such as [10, 14, 20], require the controller to update continuously at an almost infinitely high frequency, which imposes substantial communication and computational resource consumption in practical networked systems. To address this limitation, the ET control strategy was introduced [21–23]. Moreover, in practical application scenarios, some systems are subject to significant external disturbances. For example, in formation control of UAVs, factors such as wind and airflow can affect the system. Therefore, studying external disturbances is also of great importance. Some scholars have already investigated systems subject to external disturbances [24–26]. However, there are some real-world situations, such as UAV formation control, underwater robot collaborative detection, and smart-grid-distributed energy management, where we need to simultaneously consider the complex scenario of nonlinearity, time delays, external disturbances, and switching topologies. This raises a natural question: How can we construct an ET controller to guarantee FxTC tracking of delayed MASs with external disturbances under switching topologies? To this end, this paper aims to design a control protocol via an ET mechanism, ensuring that a nonlinear delayed first-order MAS with external disturbances can achieve FxTC tracking under switching topologies. The principal contributions and innovations, in contrast to existing results, are highlighted as listed below:

1) A new ET controller is presented. Compared with control protocols in [8, 20, 27], besides featuring nonlinearity, it not only guarantees system convergence but also enables lower controller update frequencies. Therefore, this method can reduce communication resource consumptions of the system.

2) Unlike the control protocols reported in [12, 13], in this article, the novelty lies in the integration of agent state delays and compensation terms. Notably, the disturbance compensation term can also ensure that the system achieves FxTC tracking. Consequently, this approach provides a simpler and effective framework for analyzing FxTC in delayed MASs.

3) In [9, 16, 22], FxTC for nonlinear MASs without external disturbances was explored, and in [8, 16, 28], the controllers were designed without an ET mechanism. In contrast to those studies, this study simultaneously considers external disturbances and an ET mechanism. Sufficient conditions are established to ensure FxTC tracking of delayed MASs under fixed and switching topologies, and Zeno behavior is excluded. Those results enrich the existing research findings in [8, 9, 16].

The organization of this article is as follows. Section 2 provides the necessary definitions, lemmas, and model description. In Section 3, first, a novel ET controller is provided, which is nonlinear and discontinuous, and then FxTC tracking is investigated for nonlinear delayed MASs in the presence of both fixed and switching topologies, respectively. Meanwhile, the explicit ST upper bound is derived. What is more, the absence of Zeno behavior is proved. In Section 4, simulation examples are provided to demonstrate the validity and advantage of the proposed results. Finally, Section 5 concludes the paper.

Notation: The following notations are adopted throughout this paper. Let $\mathcal{R}$ denote the real number set, $\mathcal{R}_+$ the positive real number set, $\mathcal{R}^N$ the N-dimensional column vector space, and $\mathcal{R}^{N\times N}$ the $N \times N$ real matrix space. For a real symmetric matrix $\mathcal{A}$, define $\lambda_{\max}(\mathcal{A})$ and $\lambda_{\min}(\mathcal{A})$ as its maximum and non-zero minimum eigenvalues, respectively. For all $z \in \mathcal{R}, q > 0$, denote $\mathrm{sgn}^q(z) = |z|^q \mathrm{sign}(z)$, and $\mathrm{sign}(\cdot)$ means the symbolic function. Furthermore, let $\|z\| = (\sum_{i=1}^N z_i^2)^{\frac{1}{2}}$ denote the 2-norm of the column vector $z = (z_1, z_2, \cdots, z_N)^{\mathrm{T}}$. The notation $\mathrm{diag}(\cdot)$ stands for a diagonal matrix. $\mathcal{N}_N$ represents the set $\{1, 2, \cdots, N\}$.

2. Background and model formulation

2.1. Algebraic graph theory

An undirected graph $\mathcal{G} = (V, E, A)$ is employed to capture the interaction topology among the N followers. The graph is composed of a node set $V = \{v_1, v_2, \cdots, v_N\}$, with v_i corresponding to the ith follower. The edge set $E = \{(v_i, v_j) \mid v_i, v_j \in V\}$ represents communication links between distinct followers. The adjacency matrix $A = (a_{ij})_{N\times N}$ encodes the connectivity of the graph, where $a_{ij} = 1$ for an existing edge $(v_i, v_j) \in E$ and $a_{ij} = 0$, otherwise, $i \neq j$. What is more, the graph $\mathcal{G}$ is supposed to be free of self-loops, namely, $a_{ii} = 0$ for all nodes $v_i \in V$. Therefore, A is a symmetric matrix. The Laplacian matrix $L = (l_{ij})_{N\times N}$ is constructed from the adjacency matrix A. Its elements are given by

$l_{ij} = -a_{ij}, i \neq j$, and $l_{ii} = \sum_{j=1, j\neq i}^{N} a_{ij}$, with $i, j \in \mathcal{N}_N$, which yields a symmetric matrix L. In addition, to describe communication links between the leader and N followers, the matrix $H = \mathrm{diag}(h_1, h_2, \cdots, h_N)$ is introduced. To be more specific, $h_i = 1$ if the ith follower is capable of receiving information from the leader; $h_i = 0$, otherwise. Let $L_H = L + H$, which combines the interactions among followers with the direct connection of the leader to the followers.

Assumption 1. *The topology graph among followers is undirected and connected. The interaction topology among one leader and N followers contains at least one directed spanning tree rooted at the leader; in addition, it is connected.*

From Assumption 1, it is straightforward to see that the leader is globally reachable, meaning it can directly transmit its information to at least one follower. Hence, there exists at least one $h_i > 0$ for $i \in \mathcal{N}_N$. Moreover, if the topology graph is undirected, the matrix L_H is positive definite.

2.2. Fundamentals for the definition and lemma

Consider the following delayed dynamical system:

$$\begin{cases} \dot{z}(t) = \Phi(t, z(t), z(t-\tau)),\ t \geq 0, \\ z_\theta = z(\theta) \in C([-\tau, 0], \mathcal{R}^N), \end{cases} \tag{2.1}$$

where $z(t) = (z_1(t), z_2(t), \cdots, z_N(t))^{\mathrm{T}} \in \mathcal{R}^N$ denotes the state vector, $z(t-\tau) = (z_1(t-\tau), z_2(t-\tau), \cdots, z_N(t-\tau))^{\mathrm{T}} \in \mathcal{R}^N$ represents the delayed state vector, τ denotes a nonnegative constant time delay. The function $\Phi : \mathcal{R}_+ \times \mathcal{R}^N \times \mathcal{R}^N \to \mathcal{R}^N$ is nonlinear and continuous, that is, it is assumed to be both Lebesgue measurable and locally bounded; θ denotes the independent variable in the initial interval $[-\tau, 0]$; z_θ represents the state value at the parameter θ; and the function $z : [-\tau, 0] \to \mathcal{R}^N$ is defined as the initial conditions.

To investigate fixed-time stability of the above dynamical system (2.1), suppose $\Phi(t, 0, 0) = 0$, for all $t > 0$. In what follows, one definition and some necessary lemmas will be recalled.

Definition 1. *[16] For $\mathcal{V}(z) : \mathcal{R}^N \to \mathcal{R}_+ \bigcup\{0\}$, if the following three conditions are filled:*

1) $\dot{\mathcal{V}}(z)$ exists for all $z \in \mathcal{R}^N$;
2) When $z \neq 0$, $\mathcal{V}(z) > 0$; otherwise, $\mathcal{V}(0) = 0$;
3) When $\| z \| \to +\infty$, $\mathcal{V}(z) \to +\infty$,

then it is said to be C-regular.

Lemma 1. *[16] Let $\mathcal{V}(z(t)) : \mathcal{R}^N \to \mathcal{R}_+ \bigcup\{0\}$ be a C-regular function. If the following differential inequality is satisfied:*

$$\dot{\mathcal{V}}(z(t)) \leq -\alpha\mathcal{V}(z(t-\tau)) - \beta\mathcal{V}^{\bar{p}}(z(t)) - \gamma\mathcal{V}^{\bar{q}}(z(t)), \tag{2.2}$$

along the trajectory of system (2.1) whenever $\mathcal{V}(z(t)) < \mathcal{V}(z(t-\tau))$ for $t \in [-\tau, 0]$, where $\alpha > 0, \beta > 0, \gamma > 0$, $0 < \bar{p} < 1$, and $\bar{q} > 1$, then the zero of system (2.1) is fixed-time stable. Moreover, the ST upper bound given by

$$\mathcal{T}_{max} = \left[\frac{1}{\alpha(\bar{q}-1)} + \frac{1}{\alpha(1-\bar{p})}\right] \ln\left[1 + \frac{\alpha}{\beta}\left(\frac{\beta}{\gamma}\right)^{\frac{1-\bar{p}}{\bar{q}-\bar{p}}}\right].$$

Lemma 2. *[9] For $\gamma_i \geq 0$, $i \in \mathcal{N}_N$, there exist the following inequalities:*

$$\left(\sum_{i=1}^{N} \gamma_i\right)^p \leq \sum_{i=1}^{N} \gamma_i^p \leq N^{1-p}\left(\sum_{i=1}^{N} \gamma_i\right)^p, 0 < p \leq 1; \;\; N^{1-q}\left(\sum_{i=1}^{N} \gamma_i\right)^q \leq \sum_{i=1}^{N} \gamma_i^q \leq \left(\sum_{i=1}^{N} \gamma_i\right)^q, q > 1.$$

Lemma 3. *[16] Let $P \in \mathcal{R}^{N\times N}$ be a positive definite matrix. For all $y, z \in \mathcal{R}^N$, there exists the following inequality:*

$$2y^{\mathrm{T}}Pz \leq y^{\mathrm{T}}Py + z^{\mathrm{T}}Pz.$$

Lemma 4. *[16] Let $Q \in \mathcal{R}^{N\times N}$ be a symmetric matrix. For all $y \in \mathcal{R}^N$, there exists the inequality*

$$\lambda_{min}(Q)y^{\mathrm{T}}y \leq y^{\mathrm{T}}Qy \leq \lambda_{max}(Q)y^{\mathrm{T}}y.$$

Lemma 5. *[29] For the undirected graph $\mathcal{G}$, for all $y \in \mathcal{R}^N$, the following equation holds:*

$$y^{\mathrm{T}}Ly = \frac{1}{2}\sum_{i,j=1}^{N} a_{ij}(y_j - y_i)^2.$$

Lemma 6. *[30] For the undirected graph $\mathcal{G}$, if the function $\Psi(\cdot,\cdot)$ fulfills*

$$\Psi(y_i, y_j) = -\Psi(y_j, y_i), i \neq j, i, j \in \mathcal{N}_N,$$

then

$$\sum_{i,j=1}^{N} a_{ij}z_i\Psi(y_j, y_i) = -\frac{1}{2}\sum_{i,j=1}^{N} a_{ij}(z_j - z_i)\Psi(y_j, y_i),$$

where $(y_1, y_2, \cdots, y_N)^{\mathrm{T}} \in \mathcal{R}^N$ and $(z_1, z_2, \cdots, z_N)^{\mathrm{T}} \in \mathcal{R}^N$.

2.3. Model description

In this subsection, leader-following nonlinear delayed MASs with external disturbances are considered. The system architecture consists of 1 leader and N followers, denoted by 0 and $1, 2, \cdots, N$, respectively. Its system dynamic model is given as follows:

$$\begin{aligned} &\dot{z}_0(t) = g(t, z_0(t)), \\ &\dot{z}_i(t) = g(t, z_i(t)) + u_i(t, z_i(t), z_i(t-\tau)) + d_i(t, z_i(t)), \; i \in \mathcal{N}_N, \end{aligned} \tag{2.3}$$

where $z_0(t), z_i(t) \in \mathcal{R}$ respectively denote the leader and ith follower's state variables; the function $g : \mathcal{R}_+ \times \mathcal{R} \to \mathcal{R}$ is nonlinear and continuous, which is known; $u_i(t, z_i(t), z_i(t-\tau))$, denoted simply as $u_i(t)$, represents the controller associated with the ith follower, which will be designed later; the variable $z_i(t-\tau)$ denotes the delayed state, with $\tau > 0$ being the communication delay; and $d_i(t, z_i(t))$ represents the disturbance affecting the ith follower, which is continuous with t and $z_i(t)$.

It should be noted that the leader system here is open-loop; its state is predetermined, unaffected by external disturbances, and does not receive any control input. In this case, the leader acts as a reference trajectory generator (e.g., uniform motion, sinusoidal motion, or a desired formation center), and the followers are tasked with tracking the leader's state. It is widely used in scenarios such as consensus tracking and formation control.

Remark 1. *For clarity of presentation, this paper discusses the case where the state variable is one-dimensional. For the multi-dimensional case of MAS states, the corresponding extension can be achieved by employing the Kronecker product operation.*

Assumption 2. *For all $y(t), z(t) \in \mathcal{R}$, a constant $l > 0$ exists, satisfying the following inequality:*

$$|g(t, y(t)) - g(t, z(t))| \leq l\,|y(t) - z(t)|\,.$$

Assumption 3. *The disturbance $d_i(t, z_i(t))$ is defined as bounded, i.e., a nonnegative constant d exists, satisfying:*

$$|d_i(t, z_i(t))| \leq d, i \in \mathcal{N}_N.$$

Remark 2. *Assumption 2 implies that the nonlinear difference is dominated by a linear error bound, thereby simplifying the application of Lyapunov methods for stability analysis. Assumption 3 is reasonable and feasible in many practical engineering scenarios. For example, when drones fly at low altitudes, they are typically affected by wind. Through meteorological data and flight environment modeling, a conservative upper bound of wind disturbance can be estimated in an engineering sense. It prevents the system from tending to infinity in finite time and facilitates the analysis of system stability by constructing Lyapunov functions.*

Definition 2. *[16] Consider the MASs (2.3) under a prescribed control protocol $u_i(t), i \in \mathcal{N}_N$. If the following conditions are satisfied:*

$$\lim_{t \to \mathcal{T}^-} |z_i(t) - z_0(t)| = 0, z_i(t) \equiv z_0(t), \forall t \geq \mathcal{T}, \forall i,$$

where $\mathcal{T} > 0$ is initial-condition-dependent, and there exists an upper bound $\mathcal{T}_{max}$ that is initial-condition-independent, then the system is said to reach FxTC tracking.

3. Main results

3.1. ET controller design

To tackle the challenges of input delay and external disturbances, an ET control protocol is developed for nonlinear MASs to reach FxTC. The designed controller is applicable to not only fixed but also switching communication topologies.

For convenience, let t_k^i represent the kth triggering time of the ith agent, $i \in \{0\} \bigcup \mathcal{N}_N$, $k = 1, 2, \cdots$. When $t \in [t_k^i, t_{k+1}^i)$, the new $u_i(t)$ is designed as follows:

$$\begin{aligned}
u_i(t) = &\sum_{j=1}^{N} a_{ij} \mathrm{sig}^q \left(z_j(t_k^i) - z_i(t_k^i)\right) - h_i \mathrm{sig}^q \left(z_i(t_k^i) - z_0(t_k^i)\right) \\
&+ \kappa_1 \left(\sum_{j=1}^{N} a_{ij} \left(z_j(t_k^i - \tau) - z_i(t_k^i - \tau)\right) - h_i \left(z_i(t_k^i - \tau) - z_0(t_k^i - \tau)\right)\right) \\
&+ \left(\kappa_2 + \kappa_3 \frac{||w^\tau(t_k^i)||^2}{||w(t_k^i)||^2 + \varepsilon}\right) \left(\sum_{j=1}^{N} a_{ij} \left(z_j(t_k^i) - z_i(t_k^i)\right) - h_i \left(z_i(t_k^i) - z_0(t_k^i)\right)\right)
\end{aligned} \tag{3.1}$$

$$+\bar{d}\left(\sum_{j=1}^{N} a_{ij}\mathrm{sig}\left(z_j(t_k^i)-z_i(t_k^i)\right)-h_i\mathrm{sig}\left(z_i(t_k^i)-z_0(t_k^i)\right)\right),$$

where $q>1$; $w(t_k^i)=(w_1(t_k^i),w_2(t_k^i),\cdots,w_N(t_k^i))^{\mathrm{T}}$ is the state tracking error vector at the triggering time t_k^i, with $w_i(t_k^i)=z_i(t_k^i)-z_0(t_k^i)$ being the tracking error of the ith follower; $w^{\tau}(t_k^i)=(w_1(t_k^i-\tau),w_2(t_k^i-\tau),\cdots,w_N(t_k^i-\tau))^{\mathrm{T}}$ is its delayed version, with $w_i(t_k^i-\tau)=z_i(t_k^i-\tau)-z_0(t_k^i-\tau)$ being the delayed tracking error, $i\in\mathcal{N}_N$; $\kappa_1,\kappa_2,\kappa_3$, and $\bar{d}$ are positive control gains to be designed; and $\varepsilon>0$ is a regularization parameter.

This design strategy ensures that control updates are triggered only when actually needed. As a result, it not only guarantees the system's stability and convergence but also significantly reduces unnecessary consumption of communication and computational resources.

Remark 3. *In controller (3.1), the term of* $\sum_{j=1}^{N} a_{ij}(z_j(t_k^i-\tau)-z_i(t_k^i-\tau))-h_i\left(z_i(t_k^i-\tau)-z_0(t_k^i-\tau)\right)$*, including the time delay of each agent's state, is designed. In the proof of Theorems 1 and 3, it is used to acquire the first term* $\mathcal{V}(z(t-\tau))$ *of inequality (2.2) in Lemma 1. Nevertheless, the existing FxTC controllers in [13, 31] do not contain the time delay of each agent's state. Thereby this is one of the improvements.*

Remark 4. *The control gains* κ_2 *and* κ_3 *play a pivotal role in compensating for system nonlinearities and the time-delayed term. The design is essential for maintaining system stability and ensuring the efficacy of the ET communication scheme. The term* $\kappa_2\left(\sum_{j=1}^{N} a_{ij}\left(z_j(t_k^i)-z_i(t_k^i)\right)-h_i\left(z_i(t_k^i)-z_0(t_k^i)\right)\right)$ *is designed to compensate for the nonlinear function. The term* $\bar{d}\left(\sum_{j=1}^{N} a_{ij}\mathrm{sig}\left(z_j(t_k^i)-z_i(t_k^i)\right)-h_i\mathrm{sig}\left(z_i(t_k^i)-z_0(t_k^i)\right)\right)$ *serves a dual purpose: it compensates for external disturbances and guarantees the realization of FxTC in the system.*

The ith follower's measurement error is designed as:

$$\begin{aligned}
E_i(t)=&-\sum_{j=1}^{N} a_{ij}\mathrm{sig}^q\left(z_j(t_k^i)-z_i(t_k^i)\right)+h_i\mathrm{sig}^q\left(z_i(t_k^i)-z_0(t_k^i)\right)\\
&-\kappa_1\left(\sum_{j=1}^{N} a_{ij}\left(z_j(t_k^i-\tau)-z_i(t_k^i-\tau)\right)-h_i\left(z_i(t_k^i-\tau)-z_0(t_k^i-\tau)\right)\right)\\
&-\left(\kappa_2+\kappa_3\frac{\|w^{\tau}(t_k^i)\|^2}{\|w(t_k^i)\|^2+\varepsilon}\right)\left(\sum_{j=1}^{N} a_{ij}\left(z_j(t_k^i)-z_i(t_k^i)\right)-h_i\left(z_i(t_k^i)-z_0(t_k^i)\right)\right)\\
&-\bar{d}\left(\sum_{j=1}^{N} a_{ij}\mathrm{sig}\left(z_j(t_k^i)-z_i(t_k^i)\right)-h_i\mathrm{sig}\left(z_i(t_k^i)-z_0(t_k^i)\right)\right)\\
&+\sum_{j=1}^{N} a_{ij}\mathrm{sig}^q\left(z_j(t)-z_i(t)\right)-h_i\mathrm{sig}^q\left(z_i(t)-z_0(t)\right)\\
&+\kappa_1\left(\sum_{j=1}^{N} a_{ij}\left(z_j(t-\tau)-z_i(t-\tau)\right)-h_i\left(z_i(t-\tau)-z_0(t-\tau)\right)\right)\\
&+\left(\kappa_2+\kappa_3\frac{\|w^{\tau}(t)\|^2}{\|w(t)\|^2+\varepsilon}\right)\left(\sum_{j=1}^{N} a_{ij}\left(z_j(t)-z_i(t)\right)-h_i\left(z_i(t)-z_0(t)\right)\right)
\end{aligned}\tag{3.2}$$

$$+\bar{d}\left(\sum_{j=1}^{N} a_{ij}\mathrm{sig}\left(z_j(t)-z_i(t)\right)-h_i\mathrm{sig}\left(z_i(t)-z_0(t)\right)\right),$$

where $w_i(t) = z_i(t) - z_0(t)$ is the ith follower's tracking error, $w(t) = (w_1(t), w_2(t), \cdots, w_N(t))^{\mathrm{T}}$ is the tracking error vector, and $w_i(t-\tau) = z_i(t-\tau) - z_0(t-\tau)$ and $w^{\tau}(t) = (w_1(t-\tau), w_2(t-\tau), \cdots, w_N(t-\tau))^{\mathrm{T}}$ are their corresponding delayed versions.

According to (3.2), controller (3.1) can be rewritten as listed below:

$$\begin{aligned} u_i(t) =& -E_i(t)+\sum_{j=1}^{N} a_{ij}\mathrm{sig}^q\left(w_j(t)-w_i(t)\right)-h_i\mathrm{sig}^q\left(w_i(t)\right)\\ &+\kappa_1\left(\sum_{j=1}^{N} a_{ij}\left(w_j(t-\tau)-w_i(t-\tau)\right)-h_iw_i(t-\tau)\right)\\ &+\left(\kappa_2+\kappa_3\frac{\|w^{\tau}(t)\|^2}{\|w(t)\|^2+\varepsilon}\right)\left(\sum_{j=1}^{N} a_{ij}\left(w_j(t)-w_i(t)\right)-h_iw_i(t)\right)\\ &+\bar{d}\left(\sum_{j=1}^{N} a_{ij}\mathrm{sig}\left(w_j(t)-w_i(t)\right)-h_i\mathrm{sig}\left(w_i(t)\right)\right). \end{aligned} \tag{3.3}$$

In view of the measurement error presented in (3.2), the ET function for the ith follower is formulated as follows:

$$F_i(t) = |E_i(t)| - \rho_i|w_i(t)|, \tag{3.4}$$

where $\rho_i \in (0, 1)$ is a selectable trigger parameter for the ith follower, $i \in \mathcal{N}_N$. Consequently, the subsequent triggering instant for the ith follower can be determined by:

$$t_{k+1}^i = \inf\left\{t > t_k^i | F_i(t) \geq 0\right\}.$$

Therefore, the update of controller (3.1) will be performed at ET instants, denoted as $t_1^i, t_2^i, \cdots, t_k^i, \cdots$. Figure 1 depicts the control schematic architecture.

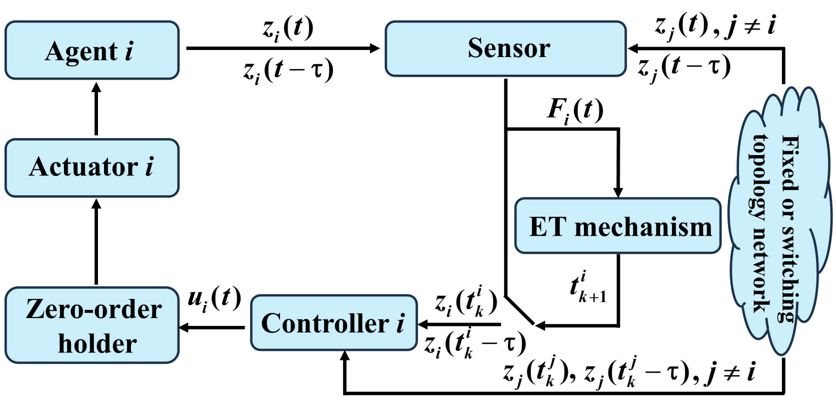

Figure 1. The control schematic architecture of the ET mechanism.

3.2. FxTC tracking under a fixed topology

In this subsection, FxTC tracking will be analyzed for delayed MASs (2.3) with external disturbances under a fixed topology.

Theorem 1. *For the MASs (2.3) under controller (3.1), if Assumptions 1, 2, and 3 are valid, the control gains κ_1, κ_2, κ_3, $\bar{d}$ and positive constant l are chosen subject to the following conditions:*

$$\kappa_3\lambda_{min}(L_H) - \kappa_1 > 0, \tag{3.5}$$

$$2\kappa_2\lambda_{min}(L_H) - 2\rho_{max} - \kappa_1\lambda^2_{max}(L_H) - 2l > 0, \tag{3.6}$$

$$\frac{\sqrt{2}}{2}\bar{d}\lambda^{\frac{1}{2}}_{min}(2L + D_{h^2}) - \sqrt{2}dN^{\frac{1}{2}} > 0. \tag{3.7}$$

Then it achieves FxTC tracking, and the ST upper bound is estimated as

$$\mathcal{T}^1_{max} = \left[\frac{2}{\alpha(q-1)} + \frac{2}{\alpha}\right]\ln\left[1 + \frac{\alpha}{\beta}\left(\frac{\beta}{\gamma}\right)^{\frac{1}{q}}\right],$$

where $\rho_{max} = \max_{1\leq i\leq N}\rho_i$, $\alpha = \kappa_3\lambda_{min}(L_H) - \kappa_1$, $\beta = \frac{\sqrt{2}}{2}\bar{d}\lambda^{\frac{1}{2}}_{min}(2L + D_{h^2}) - \sqrt{2}dN^{\frac{1}{2}}$, $\gamma = 2^{\frac{q-1}{2}}[N(N+1)]^{\frac{1-q}{2}}\lambda^{\frac{q+1}{2}}_{min}(2L + D_{\check{h}})$, $D_{h^2} = \text{diag}\left((2h_1)^2, (2h_2)^2, \cdots, (2h_N)^2\right)$, and $D_{\check{h}} = \text{diag}\left((2h_1)^{\frac{2}{q+1}}, (2h_2)^{\frac{2}{q+1}}, \cdots, (2h_N)^{\frac{2}{q+1}}\right)$.

Proof: Consider the Lyapunov function $\mathcal{V}(t)$ as:

$$\mathcal{V}(t) = \frac{1}{2}\sum_{i=1}^{N} w_i^2(t).$$

Taking the derivative of $\mathcal{V}(t)$ along (2.3), and substituting (3.3), one yields

$$\begin{aligned}
\dot{\mathcal{V}}(t) &= \sum_{i=1}^{N} w_i(t)\dot{w}_i(t) \\
&= \sum_{i=1}^{N} w_i(t)\left[u_i(t) + g(t, z_i(t)) - g(t, z_0(t)) + d_i(t, z_i(t))\right] \\
&= -\sum_{i=1}^{N} w_i(t)E_i(t) + \sum_{i=1}^{N} w_i(t)\sum_{j=1}^{N} a_{ij}\text{sig}^q\left(w_j(t) - w_i(t)\right) - \sum_{i=1}^{N} w_i(t)h_i\text{sig}^q\left(w_i(t)\right) \\
&\quad + \kappa_1\sum_{i=1}^{N} w_i(t)\left(\sum_{j=1}^{N} a_{ij}\left(w_j(t-\tau) - w_i(t-\tau)\right) - h_iw_i(t-\tau)\right) \\
&\quad + \left(\kappa_2 + \kappa_3\frac{\|w^\tau(t)\|^2}{\|w(t)\|^2+\varepsilon}\right)\sum_{i=1}^{N} w_i(t)\left(\sum_{j=1}^{N} a_{ij}\left(w_j(t) - w_i(t)\right) - h_iw_i(t)\right) \\
&\quad + \bar{d}\sum_{i=1}^{N} w_i(t)\left(\sum_{j=1}^{N} a_{ij}\text{sig}\left(w_j(t) - w_i(t)\right) - h_i\text{sig}\left(w_i(t)\right)\right) \\
&\quad + \sum_{i=1}^{N} w_i(t)\left[g(t, z_i(t)) - g(t, z_0(t))\right] + \sum_{i=1}^{N} w_i(t)d_i(t, z_i(t)).
\end{aligned} \tag{3.8}$$

Applying the ET function (3.4), we have

$$-\sum_{i=1}^{N} w_i(t)E_i(t) \leq \sum_{i=1}^{N} |w_i(t)||E_i(t)|$$

$$
\begin{aligned}
&\leq \sum_{i=1}^{N} |w_i(t)|\rho_i|w_i(t)| \\
&\leq \rho_{max} \sum_{i=1}^{N} w_i^2(t) \\
&\leq 2\rho_{max}\mathcal{V}(t).
\end{aligned} \tag{3.9}
$$

According to Lemmas 6 and 2, we obtain that

$$
\begin{aligned}
& \sum_{i=1}^{N} w_i(t) \sum_{j=1}^{N} a_{ij}\mathrm{sig}^q\left(w_j(t) - w_i(t)\right) - \sum_{i=1}^{N} w_i(t)h_i\mathrm{sig}^q\left(w_i(t)\right) \\
= \;& -\frac{1}{2}\sum_{i=1}^{N}\sum_{j=1}^{N} a_{ij}(w_j(t) - w_i(t))\mathrm{sig}^q\left(w_j(t) - w_i(t)\right) - \sum_{i=1}^{N} h_i|w_i(t)|^{q+1} \\
= \;& -\frac{1}{2}\sum_{i=1}^{N}\left[\sum_{j=1}^{N} a_{ij}|w_j(t) - w_i(t)|^{q+1} + 2h_i|w_i(t)|^{q+1}\right] \\
= \;& -\frac{1}{2}\sum_{i=1}^{N}\left[\sum_{j=1}^{N}\left(a_{ij}^{\frac{1}{q+1}}|w_j(t) - w_i(t)|\right)^{q+1} + \left((2h_i)^{\frac{1}{q+1}}|w_i(t)|\right)^{q+1}\right] \\
\leq \;& -\frac{1}{2}\left[N(N+1)\right]^{\frac{1-q}{2}}\left[\sum_{i=1}^{N}\sum_{j=1}^{N} a_{ij}^{\frac{2}{q+1}}|w_j(t) - w_i(t)|^2 + \sum_{i=1}^{N}(2h_i)^{\frac{2}{q+1}}|w_i(t)|^2\right]^{\frac{q+1}{2}}.
\end{aligned} \tag{3.10}
$$

Since $a_{ij}^{\frac{2}{q+1}} = a_{ij}$, with a_{ij} denoting the (i, j)-th entry of A, $\left(a_{ij}^{\frac{2}{q+1}}\right)_{N\times N} = A$ admits an interpretation as the adjacency matrix of a new undirected graph. From Assumption 1, it can be obtained that the new graph remains connected, and its Laplacian matrix is L. Furthermore, let $D_{\check{h}} = \mathrm{diag}\left((2h_1)^{\frac{2}{q+1}}, (2h_2)^{\frac{2}{q+1}}, \cdots, (2h_N)^{\frac{2}{q+1}}\right)$, and from Lemma 5, it follows that

$$
\sum_{i=1}^{N}\sum_{j=1}^{N} a_{ij}^{\frac{2}{q+1}}|w_j(t) - w_i(t)|^2 + \sum_{i=1}^{N}(2h_i)^{\frac{2}{q+1}}|w_i(t)|^2 = 2w^{\mathrm{T}}(t)Lw(t) + w^{\mathrm{T}}(t)D_{\check{h}}w(t). \tag{3.11}
$$

Hence, substituting equation (3.11) into inequation (3.10), by using the positive definite of $2L + D_{\check{h}}$, we obtain that

$$
\begin{aligned}
& \sum_{i=1}^{N} w_i(t) \sum_{j=1}^{N} a_{ij}\mathrm{sig}^q\left(w_j(t) - w_i(t)\right) - \sum_{i=1}^{N} w_i(t)h_i\mathrm{sig}^q\left(w_i(t)\right) \\
\leq & -\frac{1}{2}\left[N(N+1)\right]^{\frac{1-q}{2}}\left[\lambda_{min}(2L + D_{\check{h}})w^{\mathrm{T}}(t)w(t)\right]^{\frac{q+1}{2}} \\
= & -2^{\frac{q-1}{2}}\left[N(N+1)\right]^{\frac{1-q}{2}}\lambda_{min}^{\frac{q+1}{2}}(2L + D_{\check{h}})\mathcal{V}^{\frac{q+1}{2}}(t).
\end{aligned} \tag{3.12}
$$

It follows from the positive definiteness of L_H, together with Lemmas 3 and 4, that

$$
\begin{aligned}
& \kappa_1\sum_{i=1}^{N} w_i(t)\left(\sum_{j=1}^{N} a_{ij}\left(w_j(t-\tau) - w_i(t-\tau)\right) - h_iw_i(t-\tau)\right) \\
= \;& -\kappa_1 w^{\mathrm{T}}(t)L_Hw^{\tau}(t) \\
\leq \;& \frac{1}{2}\kappa_1 w^{\mathrm{T}}(t)L_H^2w(t) + \frac{1}{2}\kappa_1(w^{\tau}(t))^{\mathrm{T}}w^{\tau}(t) \\
\leq \;& \kappa_1\lambda_{max}^2(L_H)\mathcal{V}(t) + \kappa_1\mathcal{V}(t-\tau),
\end{aligned} \tag{3.13}
$$

$$
\begin{aligned}
& \left(\kappa_2+\kappa_3\frac{\|w^\tau(t)\|^2}{\|w(t)\|^2+\varepsilon}\right)\sum_{i=1}^N w_i(t)\left(\sum_{j=1}^N a_{ij}\left(w_j(t)-w_i(t)\right)-h_iw_i(t)\right)\\
= & -\left(\kappa_2+\kappa_3\frac{(w^\tau(t))^{\mathrm{T}}w^\tau(t)}{w^{\mathrm{T}}(t)w(t)+\varepsilon}\right)w^{\mathrm{T}}(t)L_Hw(t)\\
\le & -\left(\kappa_2+\kappa_3\frac{(w^\tau(t))^{\mathrm{T}}w^\tau(t)}{w^{\mathrm{T}}(t)w(t)+\varepsilon}\right)\lambda_{min}(L_H)w^{\mathrm{T}}(t)w(t)\\
= & -2\kappa_2\lambda_{min}(L_H)\mathcal{V}(t)-2\kappa_3\lambda_{min}(L_H)\mathcal{V}(t-\tau)\cdot\frac{w^{\mathrm{T}}(t)w(t)}{w^{\mathrm{T}}(t)w(t)+\varepsilon}.
\end{aligned}
$$

For a sufficiently small positive number ε, when $\|w(t)\|\ge\sqrt{\varepsilon}$, we have $\|w(t)\|^2/(\|w(t)\|^2+\varepsilon)\ge 1/2$. Therefore, from the above inequality, one has

$$
\begin{aligned}
& \left(\kappa_2+\kappa_3\frac{\|w^\tau(t)\|^2}{\|w(t)\|^2+\varepsilon}\right)\sum_{i=1}^N w_i(t)\left(\sum_{j=1}^N a_{ij}\left(w_j(t)-w_i(t)\right)-h_iw_i(t)\right)\\
\le & -2\kappa_2\lambda_{min}(L_H)\mathcal{V}(t)-\kappa_3\lambda_{min}(L_H)\mathcal{V}(t-\tau).
\end{aligned}\tag{3.14}
$$

In a similar way, one has

$$
\begin{aligned}
& \sum_{i=1}^N w_i(t)\sum_{j=1}^N a_{ij}\mathrm{sig}\left(w_j(t)-w_i(t)\right)-\sum_{i=1}^N w_i(t)h_i\mathrm{sig}\left(w_i(t)\right)\\
\le & -\frac{1}{2}\left[\lambda_{min}(2L+D_{h^2})w^{\mathrm{T}}(t)w(t)\right]^{\frac{1}{2}}\\
= & -\frac{\sqrt{2}}{2}\lambda_{min}^{\frac{1}{2}}(2L+D_{h^2})\mathcal{V}^{\frac{1}{2}}(t).
\end{aligned}\tag{3.15}
$$

Based on Assumption 2, one obtains that

$$
\sum_{i=1}^N w_i(t)\left[g(t,z_i(t))-g(t,z_0(t))\right]\le\sum_{i=1}^N w_i(t)l|z_i(t)-z_0(t)|\le 2l\mathcal{V}(t).\tag{3.16}
$$

With Assumption 3, from Lemma 2, we see that

$$
\sum_{i=1}^N w_i(t)d_i(t,z_i(t))\le d\sum_{i=1}^N|w_i(t)|=d\sum_{i=1}^N\left(|w_i(t)|^2\right)^{\frac{1}{2}}\le\sqrt{2}dN^{\frac{1}{2}}\mathcal{V}^{\frac{1}{2}}(t).\tag{3.17}
$$

Applying conditions (3.5), (3.6), and (3.7), combined with (3.9) and (3.12)–(3.17), we obtain that

$$
\begin{aligned}
\dot{\mathcal{V}}(t)\le & -\left(\kappa_3\lambda_{min}(L_H)-\kappa_1\right)\mathcal{V}(t-\tau)\\
& -2^{\frac{q-1}{2}}\left[N(N+1)\right]^{\frac{1-q}{2}}\lambda_{min}^{\frac{q+1}{2}}(2L+D_{\check{h}})\mathcal{V}^{\frac{q+1}{2}}(t)\\
& -\left(2\kappa_2\lambda_{min}(L_H)-2\rho_{max}-\kappa_1\lambda_{max}^2(L_H)-2l\right)\mathcal{V}(t)\\
& -\left(\frac{\sqrt{2}}{2}\bar{d}\lambda_{min}^{\frac{1}{2}}(2L+D_{h^2})-\sqrt{2}dN^{\frac{1}{2}}\right)\mathcal{V}^{\frac{1}{2}}(t)\\
\le & -\alpha\mathcal{V}(t-\tau)-\beta\mathcal{V}^{\frac{1}{2}}(t)-\gamma\mathcal{V}^{\frac{q+1}{2}}(t).
\end{aligned}\tag{3.18}
$$

Consequently, by virtue of Lemma 1, the MASs (2.3) are guaranteed to reach FxTC tracking, with the ST upper bound as

$$
\mathcal{T}_{max}^1=\left[\frac{2}{\alpha(q-1)}+\frac{2}{\alpha}\right]\ln\left[1+\frac{\alpha}{\beta}\left(\frac{\beta}{\gamma}\right)^{\frac{1}{q}}\right].
$$

The proof is complete.

Remark 5. *In the proof process of the above theorem, the case of* $\|w(t)\| \geq \sqrt{\varepsilon}$ *is considered. In fact, when* $\|w(t)\| < \sqrt{\varepsilon}$, $w^{\mathrm{T}}(t)w(t)/(w^{\mathrm{T}}(t)w(t)+\varepsilon) \in (0,1)$, *and* $\left(\kappa_2 + \kappa_3\|w^{\tau}(t)\|^2/(\|w(t)\|^2+\varepsilon)\right)\sum_{i=1}^{N} w_i(t)\left(\sum_{j=1}^{N} a_{ij}\left(w_j(t)-w_i(t)\right) - h_i w_i(t)\right) \leq -2\kappa_2\lambda_{min}(L_H)\mathcal{V}(t)$, *it can be proved that the system can achieve practical fixed-time consensus. In practical engineering, MASs do not achieve perfect consensus either, i.e.,* $\|w(t)\|$ *does not become exactly zero. Therefore, by choosing a sufficiently small positive number* ε, *the practical convergence accuracy can reach any satisfactory level, thus not affecting the engineering practicality of the controller.*

Remark 6. $\mathcal{T}^1_{max}$ *only relies on the corresponding control parameters, algebraic connectivity, and the number of multi-agent* N. *For example, increasing* κ_3 *or decreasing* κ_1 *makes* α *larger. The parameter* α *appears in the denominator* $\left(\frac{2}{\alpha(q-1)} + \frac{2}{\alpha}\right)$ *and also in the logarithmic term* α/β *of* $\mathcal{T}^1_{\max}$. *If we regard* q, β, *and* γ *as constants and* α *as a variable, i.e., consider* $\mathcal{T}^1_{max}$ *as a function of* α, *then taking the derivative of* $\mathcal{T}^1_{max}$ *with respect to* α, *we have* $\frac{\mathrm{d}}{\mathrm{d}\alpha}\left(\mathcal{T}^1_{max}\right) = \frac{2q}{q-1} \cdot \frac{\frac{B\alpha}{1+B\alpha} - \ln(1+B\alpha)}{\alpha^2} < 0$, *where* $B = \frac{1}{\beta}\left(\frac{\beta}{\gamma}\right)^{\frac{1}{q}} = \beta^{\frac{1-q}{q}}\gamma^{-\frac{1}{q}} > 0$. *Hence, the larger* α *is, the smaller* $\mathcal{T}^1_{\max}$ *becomes (faster convergence). Similarly, increasing* $\bar{d}$ *or decreasing* d *makes* β *larger. Since* β *appears in* α/β *and* $(\beta/\gamma)^{1/q}$, *the larger* β *is, the smaller* α/β *becomes, while* $(\beta/\gamma)^{1/q}$ *becomes larger. Their product is* $\frac{\alpha}{\beta}\left(\frac{\beta}{\gamma}\right)^{1/q} = \frac{\alpha}{\beta^{1-1/q}\gamma^{1/q}}$. *Since* $1 - 1/q > 0$, *increasing* β *decreases this product, which in turn reduces the term inside the logarithm, leading to a smaller* $\mathcal{T}^1_{\max}$. *Hence, as can be inferred from* $\mathcal{T}^1_{max}$, *the consensus rate of the MASs increases with larger values of the parameters* κ_3 *and* $\bar{d}$. *However, the larger* κ_3 *and* $\bar{d}$ *are corresponds to the larger control inputs. Therefore, when choosing the parameters, the convergence rate and the control cost should be considered simultaneously.*

Remark 7. *In Theorem 1, the selection of these parameter values (gains* κ_1, κ_2, κ_3, $\bar{d}$, *disturbance bound* d, *topology eigenvalue* $\lambda_{min}(L_H)$, *and constant* l, *etc.) is crucial for the validity. For example, if* κ_3 *is too small or* κ_1 *is too large, leading to the failure of inequality (3.5), then* $\alpha \leq 0$. *The negative definite term in the Lyapunov derivative disappears, and the system may lose FxTC convergence or even diverge. If* $\bar{d}$ *is too small or* d *is too large, causing inequality (3.7) not to hold, then it can result in insufficient cancellation of the system disturbance. On the other hand, it can cause the loss of the term with a power less than one in the Lyapunov derivative, thereby potentially making the system lose FxTC convergence.*

Theorem 2. *For the nonlinear delayed MASs (2.3), under controller (3.1) and ET function (3.4), Zeno behavior is avoided. The minimum inter-event time is given by the following equation:*

$$t^i_{min} = \tau^i_k = \frac{\rho_{max}}{\hat{\xi} + \rho_{max}\hat{\xi}}. \tag{3.19}$$

Proof: When $t \in [0, \mathcal{T}^1_{max})$, define $\xi(t) = \|E(t)\|/(\|w(t)\| + \varepsilon)$, where $E(t) = (E_1(t), E_2(t), \cdots, E_N(t))^{\mathrm{T}}$, $\varepsilon > 0$.

Let

$$\begin{aligned} U_i(t) = &\sum_{j=1}^{N} a_{ij}\mathrm{sig}^q\left(z_j(t) - z_i(t)\right) - h_i\mathrm{sig}^q\left(z_i(t) - z_0(t)\right) \\ &+ \kappa_1\left(\sum_{j=1}^{N} a_{ij}\left(z_j(t-\tau) - z_i(t-\tau)\right) - h_i\left(z_i(t-\tau) - z_0(t-\tau)\right)\right) \end{aligned} \tag{3.20}$$

$$+\left(\kappa_2+\kappa_3\frac{\|w^{\tau}(t)\|^2}{\|w(t)\|^2+\varepsilon}\right)\left(\sum_{j=1}^{N}a_{ij}\left(z_j(t)-z_i(t)\right)-h_i\left(z_i(t)-z_0(t)\right)\right)$$
$$+\bar{d}\left(\sum_{j=1}^{N}a_{ij}\mathrm{sig}\left(z_j(t)-z_i(t)\right)-h_i\mathrm{sig}\left(z_i(t)-z_0(t)\right)\right),$$

and it represents the control protocol for MASs (2.3) in the case where an ET mechanism is absent.

For every time interval $[t_k^i, t_{k+1}^i), k=1,2,\cdots$, differentiating $\xi(t)$ with respect to t leads to

$$\dot{\xi}(t)=\frac{E^{\mathrm{T}}(t)\dot{E}(t)}{\|E(t)\|(\|w(t)\|+\varepsilon)}-\frac{\|E(t)\|w^{\mathrm{T}}(t)\dot{w}(t)}{\|w(t)\|(\|w(t)\|+\varepsilon)^2}=\frac{E^{\mathrm{T}}(t)\dot{U}(t)}{\|E(t)\|(\|w(t)\|+\varepsilon)}-\frac{\|E(t)\|w^{\mathrm{T}}(t)\dot{w}(t)}{\|w(t)\|(\|w(t)\|+\varepsilon)^2},\tag{3.21}$$

where the vector $U(t)=(U_1(t),U_2(t),\cdots,U_N(t))^{\mathrm{T}}$.

In Theorem 1, it has been proved that FxTC tracking is attainable for the nonlinear delayed MASs (2.3) via the proposed controller (3.1). In contrast to control protocol (3.1), the controller $U_i(t)$ updates its control input continuously in real time. Therefore, it is more conservative. It is straightforward to verify that MASs (2.3) can also reach FxTC tracking by $U_i(t)$. Since the convergence time $\mathcal{T}^1_{max}$ is a finite value and the trajectories of states $z_i(t)$ and $z_i(t-\tau)$ are continuous on $[0,\mathcal{T}^1_{max})$, the states are bounded. Since $U_i(t)$ is a function of the states and the graph topology is fixed, $U_i(t)$ is bounded. $\dot{U}_i(t)$ contains the first-order derivatives of the state variables; together with Assumptions 2 and 3, it follows that $\dot{U}_i(t)$ is also bounded. Define $U_{max}(t)=\max_{t\in[t_k^i,t_{k+1}^i)}\left\{\|\dot{U}(t)\|\right\}$, and then

$$\begin{aligned}\dot{\xi}(t)&\le\frac{U_{max}(t)}{\|w(t)\|+\varepsilon}+\xi(t)\frac{\|\dot{w}(t)\|}{\|w(t)\|+\varepsilon}\\&\le(1+\xi(t))\frac{U_{max}(t)}{\|w(t)\|+\varepsilon}+(1+\xi(t))\frac{\|\dot{w}(t)\|}{\|w(t)\|+\varepsilon}\\&\le(1+\xi(t))\left(\frac{U_{max}(t)}{\|w(t)\|+\varepsilon}+\frac{\|E(t)\|+U_{max}+l\|w(t)\|+d}{\|w(t)\|+\varepsilon}\right)\\&=(1+\xi(t))\left(\frac{2U_{max}(t)}{\|w(t)\|+\varepsilon}+l+\frac{d}{\|w(t)\|+\varepsilon}+\xi(t)\right)\\&\le\left(1+\frac{2U_{max}(t)}{\|w(t)\|+\varepsilon}+l+\frac{d}{\|w(t)\|+\varepsilon}+\xi(t)\right)^2.\end{aligned}\tag{3.22}$$

Since $\|w(t)\|=\sqrt{w^{\mathrm{T}}(t)w(t)}=\sqrt{2\mathcal{V}(t)}\le\sqrt{2\mathcal{V}(0)}$, therefore, $1+2U_{max}(t)/(\|w(t)\|+\varepsilon)+l+d/(\|w(t)\|+\varepsilon)$ must have a maximum value. Without loss of generality, suppose that its maximum value is $\hat{\xi}$, and then we have

$$\dot{\xi}(t)\le\left(\hat{\xi}+\xi(t)\right)^2.\tag{3.23}$$

Let

$$\dot{\psi}_i(t)=\left(\hat{\xi}+\psi_i(t)\right)^2,\psi_i(t_k^i)=\psi_0^i=0.\tag{3.24}$$

Then, $\xi(t)\le\psi_i(t,\psi_0^i)$, with $\psi_i(t,\psi_0^i)$ being the solution of (3.24), which is easily solved by

$$\psi_i(t,\psi_0^i)=\frac{\hat{\xi}}{1-\hat{\xi}(t-t_k^i)}-\hat{\xi}.\tag{3.25}$$

When $t = t^i_{k+1} = t^i_k + \tau^i_k$, combining with (3.24) and (3.25), one has

$$\xi(t) \le \psi_i(t, \psi^i_0) = \int_{t^i_k}^{t^i_{k+1}} \dot{\psi}_i(t, \psi^i_0)\mathrm{d}t = \int_{t^i_k}^{t^i_k+\tau^i_k} \dot{\psi}_i(t, \psi^i_0)\mathrm{d}t = \frac{\hat{\xi}\tau^i_k}{1-\hat{\xi}\tau^i_k}. \tag{3.26}$$

According to the ET function (3.4), we have that

$$\frac{\|E(t)\|}{\|w(t)\| + \varepsilon} = \frac{\sqrt{\sum_i^N E_i^2(t)}}{\|w(t)\| + \varepsilon} \le \frac{\sqrt{\sum_i^N \rho_i^2 w_i^2(t)}}{\|w(t)\| + \varepsilon} \le \frac{\rho_{max}\|w(t)\|}{\|w(t)\| + \varepsilon} \le \frac{\rho_{max}(\|w(t)\| + \varepsilon)}{\|w(t)\| + \varepsilon} = \rho_{max}. \tag{3.27}$$

Therefore, based on (3.23), (3.24), and (3.27), by the comparison principle, when $t \in \left[t^i_k, t^i_{k+1}\right)$, one has

$$\psi_i(t, \psi^i_0) = \rho_{max}. \tag{3.28}$$

Combining with (3.26) and (3.28), we have the minimum value of the triggered time interval given by (3.19), namely, for every time interval, there exists a positive inter-event lower bound. The proof is complete.

3.3. FxTC tracking under switching topologies

In real-world systems, the emergence of new communication links is often induced by agents' migration and evolution. Such dynamic uncertainties can result in the creation or dissolution of network edges. Consequently, it is imperative to account for time-varying communication topologies. Motivated by this fact, the previously derived ET control strategy established for fixed topology is generalized to the switching topologies scenario. Under switching topologies, the ET FxTC tracking controller and triggering function are similar to the fixed topology scenario. The corresponding results are presented as follows.

Consider that all possible communication topologies for the nonlinear MASs (2.3) are represented by a set of connected undirected graphs $\mathcal{G}_s = \{\mathcal{G}_1, \mathcal{G}_2, \cdots, \mathcal{G}_M\}$, where the positive integer M denotes the number of switching communication topologies. Let $\Gamma = \{1, 2, \cdots, M\}$ be the index set of the graph set, and the topology remains invariant within the intervals between switching instants. Here, we assume that each subgraph is connected. For convenience, the variation is characterized by a switching signal $h(t) : [0, +\infty) \to \Gamma$, and then the communication topology graph is denoted as $\mathcal{G}_{h(t)}$ at time t, which is the graph indexed by $h(t)$ in the graph set $\mathcal{G}_s$, and its corresponding Laplacian matrix is $L(\mathcal{G}_{h(t)})$. Let $\lambda_2^{\min}(L(\mathcal{G}_{h(t)})) = \min\{\lambda_2(L(\mathcal{G}_{h(t)}))\}$, which denotes the smallest nonzero eigenvalue of $L(\mathcal{G}_{h(t)})$. Set $L_H(\mathcal{G}_{h(t)}) = L(\mathcal{G}_{h(t)}) + H_{h(t)}$, where $H_{h(t)}$ represents the leader matrix at switching signal $h(t)$, $\hat{\lambda}_{\min}(L_H(\mathcal{G}_{h(t)})) = \min\{\lambda_{\min}(L_H(\mathcal{G}_{h(t)}))\}$, and $\hat{\lambda}_{\max}(L_H(\mathcal{G}_{h(t)})) = \max\{\lambda_{\max}(L_H(\mathcal{G}_{h(t)}))\}$.

Theorem 3. *For the MASs (2.3) under control protocol (3.1), if Assumptions 1, 2, and 3 are valid, and positive constants κ_1, κ_2, κ_3, $\bar{d}$, and l are chosen subject to the following conditions:*

$$\kappa_3\hat{\lambda}_{min}(L_H(\mathcal{G}_{h(t)})) - \kappa_1 > 0, \tag{3.29}$$

$$2\kappa_2\hat{\lambda}_{min}(L_H(\mathcal{G}_{h(t)})) - 2\rho_{max} - \kappa_1\hat{\lambda}^2_{max}(L_H(\mathcal{G}_{h(t)})) - 2l > 0, \tag{3.30}$$

$$\frac{\sqrt{2}}{2}\bar{d}\hat{\lambda}_{min}^{\frac{1}{2}}(2L(\mathcal{G}_{h(t)}) + D_{h^2}(\mathcal{G}_{h(t)})) - \sqrt{2}dN^{\frac{1}{2}} > 0, \tag{3.31}$$

then it reaches FxTC tracking, and the ST upper bound is estimated as:

$$\mathcal{T}_{max}^2 = \left[\frac{2}{\tilde{\alpha}(q-1)} + \frac{2}{\tilde{\alpha}}\right]\ln\left[1 + \frac{\tilde{\alpha}}{\tilde{\beta}}\left(\frac{\tilde{\beta}}{\tilde{\gamma}}\right)^{\frac{1}{q}}\right],$$

where $\tilde{\alpha} = \kappa_3\hat{\lambda}_{min}(L_H(\mathcal{G}_{h(t)})) - \kappa_1$, $\tilde{\beta} = \frac{\sqrt{2}}{2}\bar{d}\hat{\lambda}_{min}^{\frac{1}{2}}(2L(\mathcal{G}_{h(t)}) + D_{h^2}(\mathcal{G}_{h(t)})) - \sqrt{2}dN^{\frac{1}{2}}$, $\tilde{\gamma} = 2^{\frac{q-1}{2}}[N(N+1)]^{\frac{1-q}{2}}\hat{\lambda}_{min}^{\frac{q+1}{2}}(2L(\mathcal{G}_{h(t)}) + D_{\check{h}}(\mathcal{G}_{h(t)}))$, $D_{h^2}(\mathcal{G}_{h(t)})$ and $D_{\check{h}}(\mathcal{G}_{h(t)})$ denote the diagonal matrices at switching signal $h(t)$, respectively, representing the leader and followers' connection relationship, $\hat{\lambda}_{min}(2L(\mathcal{G}_{h(t)}) + D_{h^2}(\mathcal{G}_{h(t)})) = \min\{\lambda_{min}(2L(\mathcal{G}_{h(t)}) + D_{h^2}(\mathcal{G}_{h(t)}))\}$, and $\hat{\lambda}_{min}(2L(\mathcal{G}_{h(t)}) + D_{\check{h}}(\mathcal{G}_{h(t)})) = \min\{\lambda_{min}(2L(\mathcal{G}_{h(t)}) + D_{\check{h}}(\mathcal{G}_{h(t)}))\}$.

Proof: Consider the following Lyapunov function:

$$\mathcal{V}(t) = \frac{1}{2}\sum_{i=1}^{N} w_i^2(t).$$

By an argument analogous to Theorem 1, using the ET controller (3.1) together with triggering function (3.4), $\dot{\mathcal{V}}(t)$ can be computed by

$$\begin{aligned}
\dot{\mathcal{V}}(t) \leq\ & -\left(\kappa_3\hat{\lambda}_{min}(L_H(\mathcal{G}_{h(t)})) - \kappa_1\right)\mathcal{V}(t-\tau) \\
& - 2^{\frac{q-1}{2}}[N(N+1)]^{\frac{1-q}{2}}\hat{\lambda}_{min}^{\frac{q+1}{2}}(2L(\mathcal{G}_{h(t)}) + D_{\check{h}}(\mathcal{G}_{h(t)}))\mathcal{V}^{\frac{q+1}{2}}(t) \\
& - \left(2\kappa_2\hat{\lambda}_{min}(L_H(\mathcal{G}_{h(t)})) - 2\rho_{max} - \kappa_1\hat{\lambda}_{max}^2(L_H(\mathcal{G}_{h(t)})) - 2l\right)\mathcal{V}(t) \\
& - \left(\frac{\sqrt{2}}{2}\bar{d}\hat{\lambda}_{min}^{\frac{1}{2}}(2L(\mathcal{G}_{h(t)}) + D_{h^2}(\mathcal{G}_{h(t)})) - \sqrt{2}dN^{\frac{1}{2}}\right)\mathcal{V}^{\frac{1}{2}}(t) \\
\leq\ & -\tilde{\alpha}\mathcal{V}(t-\tau) - \tilde{\beta}\mathcal{V}^{\frac{1}{2}}(t) - \tilde{\gamma}\mathcal{V}^{\frac{q+1}{2}}(t).
\end{aligned} \tag{3.32}$$

Obviously, for all $h(t) \in \Gamma$, the above inequality holds. According to Lemma 1, it can be easily verified that MASs (2.3) achieves FxTC, and the ST upper bound is given by $\mathcal{T}_{max}^2$. The proof is complete.

Remark 8. *Unlike the existing results [9, 18, 28], these results extend to nonlinear delayed leader-follower MASs under switching topologies. Furthermore, the findings reported in [15, 16, 22] are encompassed as special cases of the more general results derived in this article.*

Remark 9. *The investigation of nonlinear MASs subject to time delay and switching topologies based on the ET mechanism is of substantial practical value, with applications including UAV formation control, underwater robot collaborative detection, and smart-grid-distributed energy management. For instance, in UAV formation cooperative control, multiple UAVs are required to maintain formation during flight, yet communication is affected by weather, obstacles, or distance, leading to dynamically switching topologies. Meanwhile, signal transmission among UAVs suffers from time delays and flight is influenced by aerodynamic nonlinearities. In addition, continuous control methods impose high demands on communication bandwidth, which leads to a high update frequency of the controller and consumes a large amount of communication resources. Consequently, in order to lower energy consumption, enhance consensus performance, and preserve formation stability, an ET mechanism, time delays, and switching topologies are critical issues to address in FxTC of MASs.*

Theorem 4. *For MASs (2.3), under controller (3.1) and ET function (3.4), Zeno behavior is excluded.*

Proof: By an argument analogous to Theorem 2, it follows that there is no Zeno behavior. This completes the proof.

4. Simulation results

Example 1. Simulation on a nonlinear delayed MAS: Consider nonlinear delayed MASs with external disturbances under switching topologies, which involve one leader denoted as 0 and 5 followers denoted as 1–5. Figure 2 shows three switching topologies $\mathcal{G}_1$, $\mathcal{G}_2$, and $\mathcal{G}_3$, which are connected undirected graphs. From Figure 2, we have $h_1 = h_3 = h_4 = 1$ and $h_2 = h_5 = 0$ in graphs $\mathcal{G}_1$ and $\mathcal{G}_2$, while $h_1 = h_3 = 1$ and $h_2 = h_4 = h_5 = 0$ in graph $\mathcal{G}_3$. For each switching topology $\mathcal{G}_i$, the adjacency matrix A_i and matrix L_{H_i} $(i = 1, 2, 3)$ are respectively listed as follows:

$$A_1 = \begin{pmatrix} 0 & 1 & 0 & 1 & 0 \\ 1 & 0 & 0 & 0 & 1 \\ 0 & 0 & 0 & 1 & 0 \\ 1 & 0 & 1 & 0 & 1 \\ 0 & 1 & 0 & 1 & 0 \end{pmatrix}, L_{H_1} = \begin{pmatrix} 3 & -1 & 0 & -1 & 0 \\ -1 & 2 & 0 & 0 & -1 \\ 0 & 0 & 2 & -1 & 0 \\ -1 & 0 & -1 & 4 & -1 \\ 0 & -1 & 0 & -1 & 2 \end{pmatrix},$$

$$A_2 = \begin{pmatrix} 0 & 1 & 0 & 0 & 1 \\ 1 & 0 & 0 & 0 & 1 \\ 0 & 0 & 0 & 1 & 0 \\ 0 & 0 & 1 & 0 & 1 \\ 1 & 1 & 0 & 1 & 0 \end{pmatrix}, L_{H_2} = \begin{pmatrix} 3 & -1 & 0 & 0 & -1 \\ -1 & 2 & 0 & 0 & -1 \\ 0 & 0 & 2 & -1 & 0 \\ 0 & 0 & -1 & 3 & -1 \\ -1 & -1 & 0 & -1 & 3 \end{pmatrix},$$

$$A_3 = \begin{pmatrix} 0 & 1 & 0 & 1 & 0 \\ 1 & 0 & 0 & 0 & 1 \\ 0 & 0 & 0 & 1 & 0 \\ 1 & 0 & 1 & 0 & 1 \\ 0 & 1 & 0 & 1 & 0 \end{pmatrix}, L_{H_3} = \begin{pmatrix} 3 & -1 & 0 & -1 & 0 \\ -1 & 2 & 0 & 0 & -1 \\ 0 & 0 & 2 & -1 & 0 \\ -1 & 0 & -1 & 3 & -1 \\ 0 & -1 & 0 & -1 & 2 \end{pmatrix}.$$

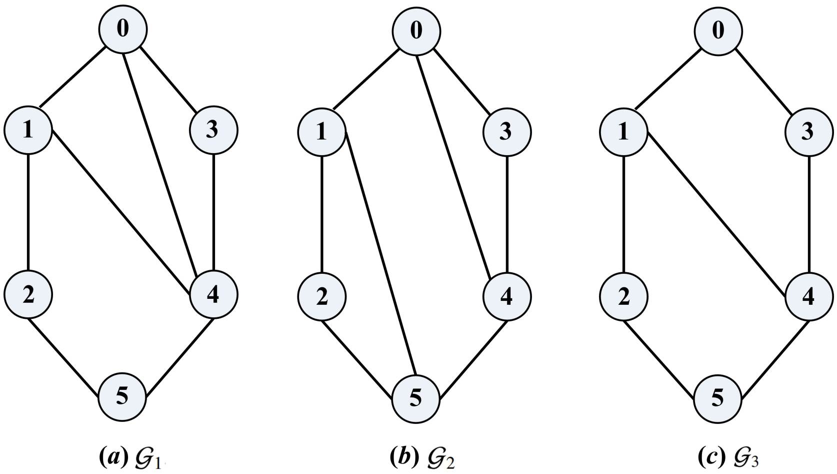

Figure 2. Switching topologies of leader-following MASs.

The nonlinear dynamics of MASs are described as (2.3), with the ith follower's controller $u_i(t)$ given by (3.1). Set $g(t, z_i(t)) = 0.2z_i(t) - 0.2\sin(t)$, $i = 0, 1, 2, 3, 4, 5$. The external disturbance $d_i(t, z_i(t)) = 0.2\cos(z_i(t))$, $i = 1, 2, 3, 4, 5$. One can easily confirm that $g(t, z_i(t))$ fulfills Assumption 2, where the constant l is taken as 0.2, and $d_i(t, z_i(t))$ fulfills Assumption 3 with the constant $d = 0.2$. Suppose that the information of the initial state for each agent is selected as $z_0(0) = 1, z_1(0) = 4, z_2(0) = 6, z_3(0) = -1, z_4(0) = -3, z_5(0) = 2$. According to the tracking control protocol (3.1), the control gains are set as $\kappa_1 = 0.1, \kappa_2 = 6.48, \kappa_3 = 1.05, \bar{d} = 1.2$, and the other parameters are set as $q = 2.12$, $\tau = 0.05$, $\rho_i = 0.5, i = 1, 2, 3, 4, 5$. Thus far, by some simple calculations, we obtain that $\hat{\lambda}_{min}(L_H(\mathcal{G}_{h(t)})) = 0.2841$, $\hat{\lambda}_{max}(L_H(\mathcal{G}_{h(t)})) = 5.2717$, $\hat{\lambda}_{min}(2L(\mathcal{G}_{h(t)}) + D_{h^2}(\mathcal{G}_{h(t)})) = 0.8518$, $\hat{\lambda}_{min}(2L(\mathcal{G}_{h(t)}) + D_{\check{h}}(\mathcal{G}_{h(t)})) = 0.4758$. Thus, it has been verified that conditions (3.29)–(3.31) in Theorem 3 hold. Therefore, FxTC tracking is reached. Furthermore, the ST upper bound can be evaluated as $\mathcal{T}^2_{max} = 7.0765$ s.

In the numerical simulation, system (2.3) starts with topology graph $\mathcal{G}_1$, switches to topology graph $\mathcal{G}_2$ at $t = 0.3$ s, and then changes to topology graph $\mathcal{G}_3$ at $t = 0.6$ s. All agent profiles are given in Figures 3–6. Figure 3 displays the leader and followers' state trajectories with controller (3.1). It is easy to observe that the five followers achieve FxTC tracking within 0.6 s, and the actual ST meets the requirement of the ST upper bound $\mathcal{T}^2_{max}$. In addition, the five followers ultimately achieve consensus with the leader. Figure 4 shows every follower's tracking error $z_i(t) - z_0(t)$ trajectory. The control input trajectories of the five followers are illustrated in Figure 5. What is more, from Figures 3–5, it can further be noted that not only does the system reach consensus when the communication topologies switch, but also the state trajectories, tracking error trajectories, and control inputs change at the time instant $t = 0.3$ s. Figure 6 depicts the inter-event intervals of the followers. From it, one can observe that under the proposed controller, the triggering frequency remains relatively low during the system convergence stage, and Zeno behavior is avoided, which is consistent with Theorem 4. Therefore, the ET mechanism considerably decreases communication frequency, thus reducing resource consumption without compromising performance.

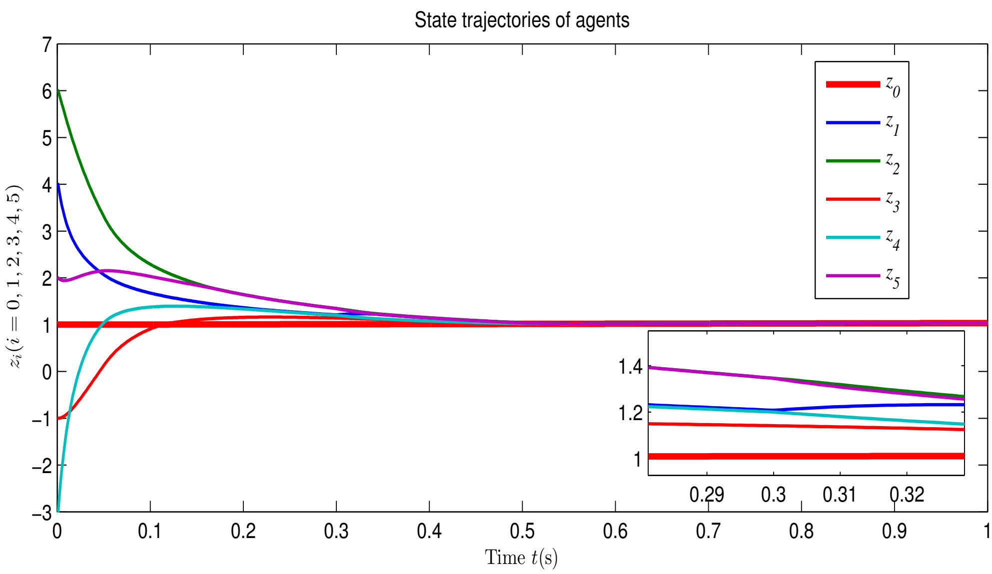

Figure 3. State trajectories with $\tau = 0.05$ and controller (3.1) under switching topologies.

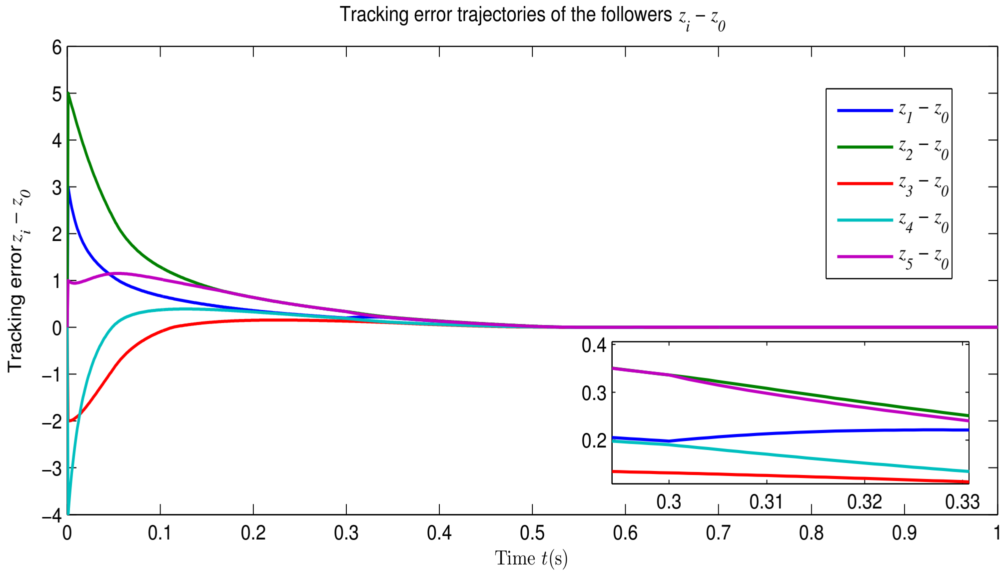

Figure 4. Tracking error trajectories with controller (3.1) under switching topologies.

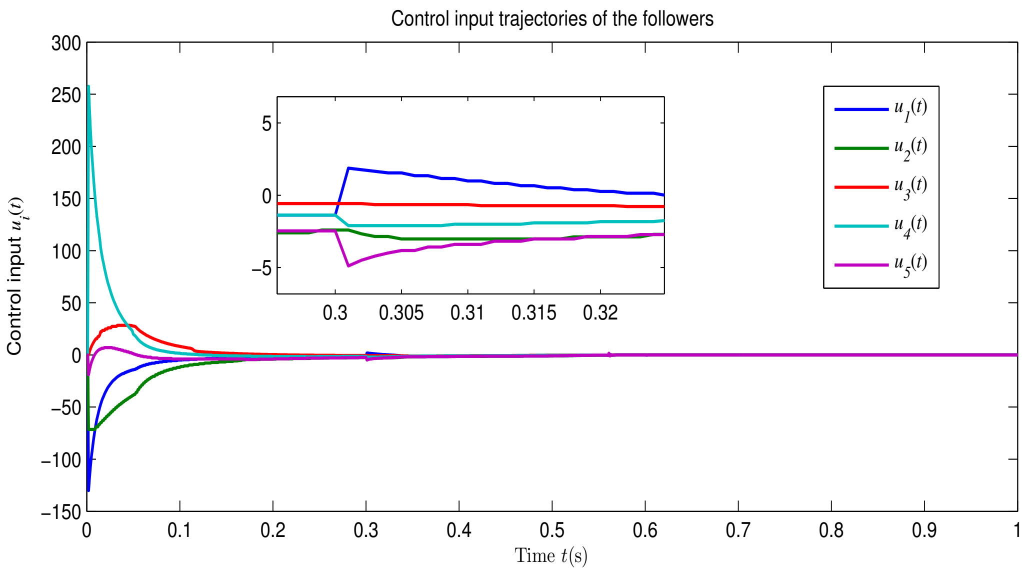

Figure 5. Control input of each follower under switching topologies.

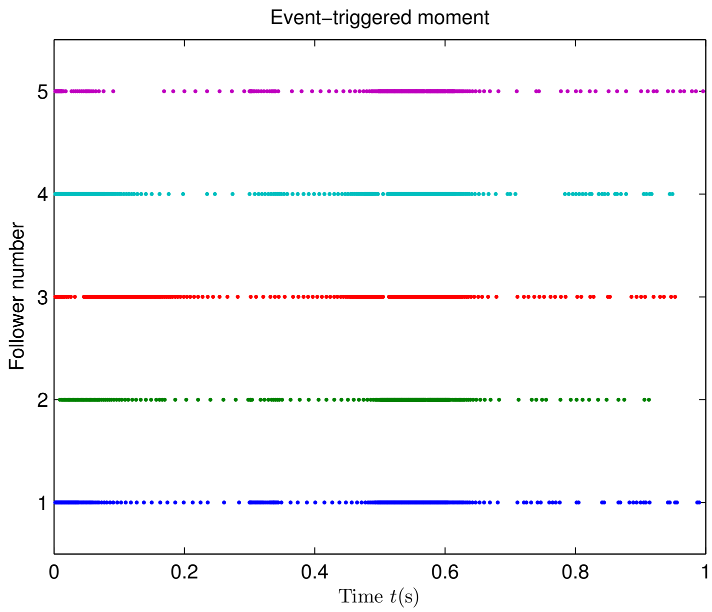

Figure 6. Triggering instants of followers with controller (3.1) under switching topologies.

When $\tau = 0.1$ s under the same initial states, the same control gains $\kappa_1, \kappa_2, \kappa_3, \bar{d}$, and the same other parameters q, $\rho_i, i = 1, 2, 3, 4, 5$, the simulation result is shown in Figure 7. It can be seen from this figure that the trajectories of the leader and followers reach consensus under control protocol (3.1) and ET function (3.4). When $\tau = 0.2$ with $\kappa_1 = 0.01$, $\kappa_2 = 3.88$, and $\rho_i = 0.65$, the simulation result is given in Figure 8. As τ increases ($0.05 \rightarrow 0.1 \rightarrow 0.2$), the ST increases slightly, but still remains below the theoretical upper bound. Moreover, it can also be observed that the time delay affects the consensus time of the system, and the reason is that the controller contains the time delay.

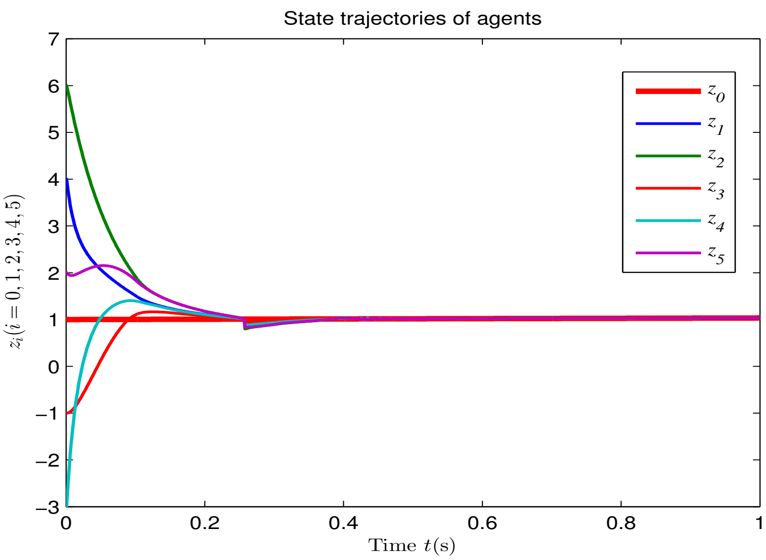

Figure 7. State trajectories with $\tau = 0.1$ and controller (3.1) under switching topologies.

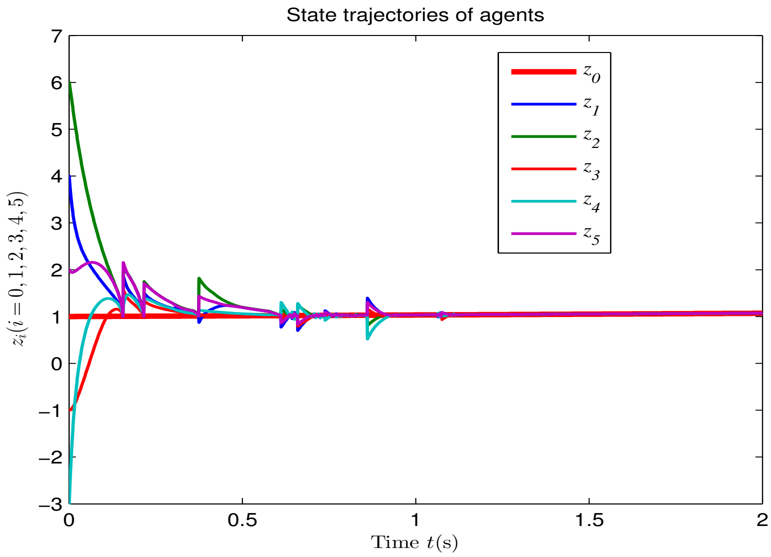

Figure 8. State trajectories with $\tau = 0.2$ and controller (3.1) under switching topologies.

Remark 10. *In numerical simulations, we take* $\tau = 0.05$ *and* 0.1 *as examples under the same initial state, control gains, and other parameters; while when taking* $\tau = 0.2$*, some values of control gains or other parameters need to be adjusted for the system to achieve FxTC tracking. Different values of* τ *yield different ST upper bounds. This implies that time delay affects the time of system consensus.*

To demonstrate disturbance rejection, some numerical simulations are performed with different values of d. However, when d takes different values, according to the conditions in Theorems 1 and 3, the control gains and other parameters need to be adjusted accordingly to achieve consensus. Next, we perform numerical simulations with $d = 0.5$, $\bar{d} = 2.5$ and $d = 1$, $\bar{d} = 4.85$ under the same other parameter values with $\tau = 0.05$, and the results are shown in Figures 9 and 10, respectively. When d and $\bar{d}$ change, they affect the value of β, thereby influencing the upper bound of the ST.

In order to verify the impact of topology switching on system consensus, the switching interval is adjusted to 0.1 second under the same conditions and let the topologies $\mathcal{G}_1$, $\mathcal{G}_2$, and $\mathcal{G}_3$ appear cyclically. In other words, system (2.3) starts with topology graph $\mathcal{G}_1$, switches to topology graph $\mathcal{G}_2$ at $t = 0.1$ s, changes to topology graph $\mathcal{G}_3$ at $t = 0.2$ s, then changes to topology graph $\mathcal{G}_1$ at $t = 0.3$ s, and so on. The corresponding numerical simulation results are shown in Figure 11. It can be observed from the figure that although the switching frequency increases, the system consensus is not affected, which further validates the effectiveness of the proposed controller and ET mechanism.

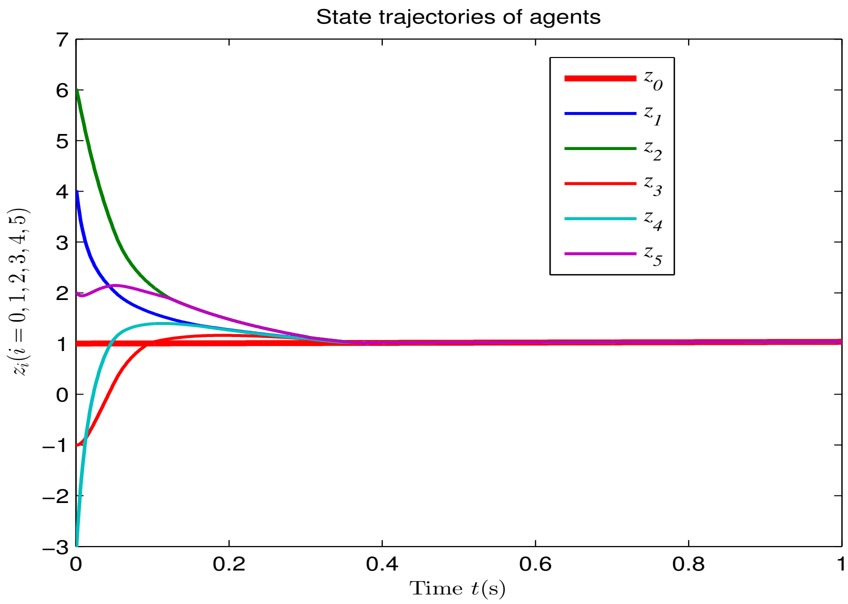

Figure 9. State trajectories with $d = 0.5$ and controller (3.1) under switching topologies.

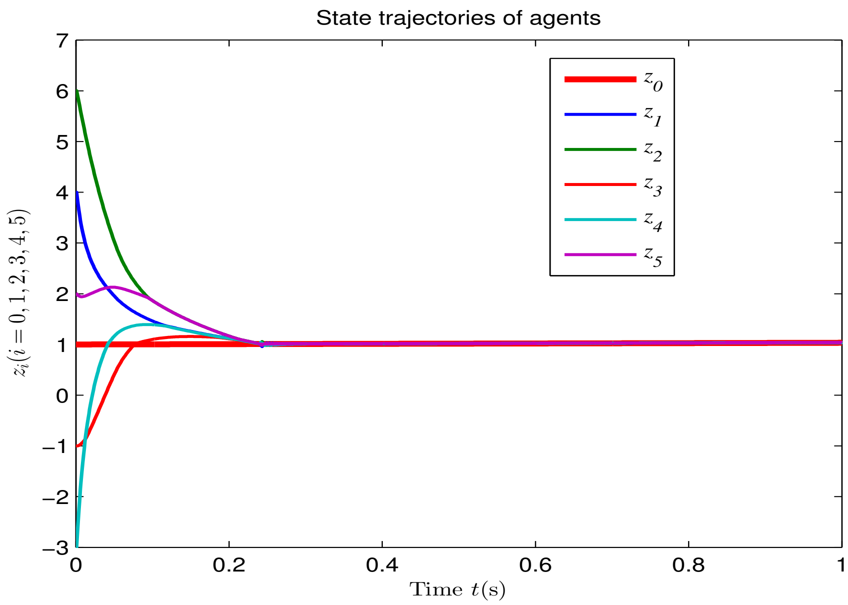

Figure 10. State trajectories with $d = 1.0$ and controller (3.1) under switching topologies.

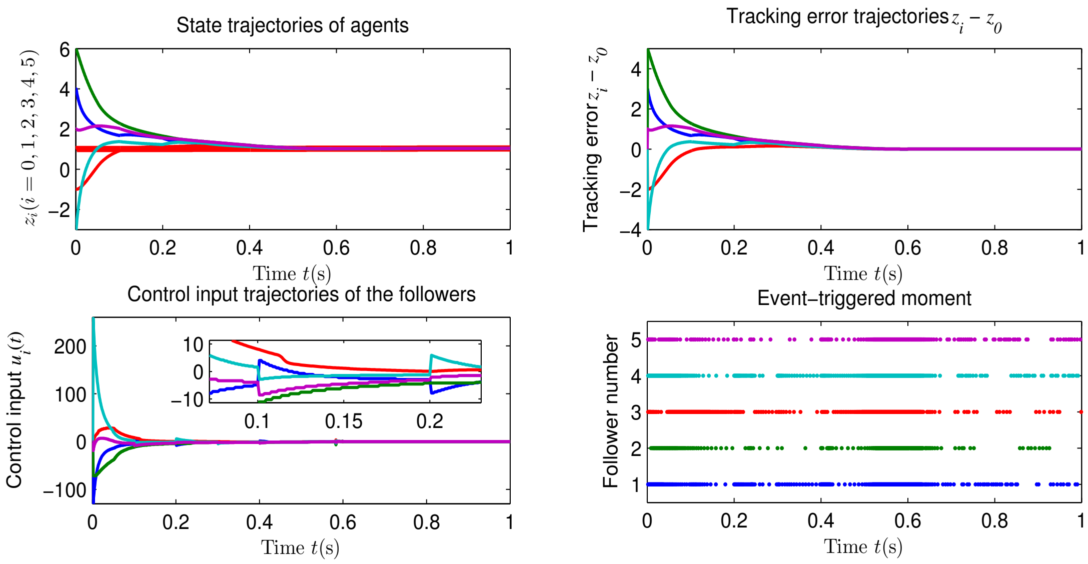

Figure 11. Simulation results of topology switching every 0.1 second.

To further validate the advantages of the designed ET control algorithm, a comparative analysis with the algorithm in [25] is carried out on the basis of the aforementioned numerical simulation. Since the considered undirected graphs are different, the proposed controllers differ accordingly. In the numerical simulation, for fairness, only the controller design method in [25] is adopted, and the experiment is conducted only under the communication topology graph $\mathcal{G}_1$, without considering the leader controller in [25] and the time delay involved in this paper. Furthermore, the controller parameters given in [25] are maintained to be consistent with the original reference. Figures 12 and 13 display the simulation results. It is found that the control input chattering amplitude of the ET controller proposed in this article is relatively smaller, which can mitigate hardware damage to some extent in practical scenarios. In addition, the number of ET mechanisms in this paper is significantly lower than that in reference [25]. Therefore, the ET controller designed in this work has greater advantages in reducing system energy consumption, and can reduce system resource waste to some extent in real-world applications.

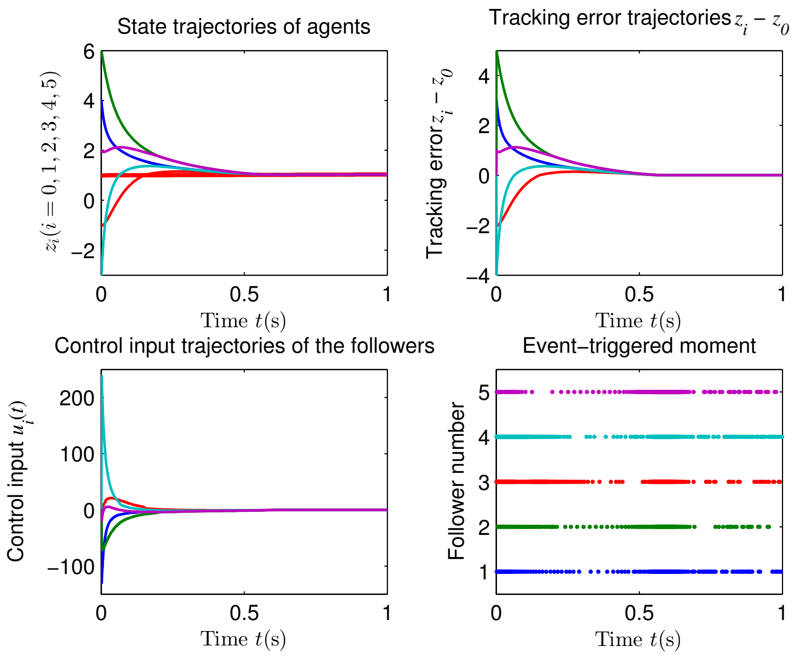

Figure 12. Simulation results with controller (3.1) under $\mathcal{G}_1$.

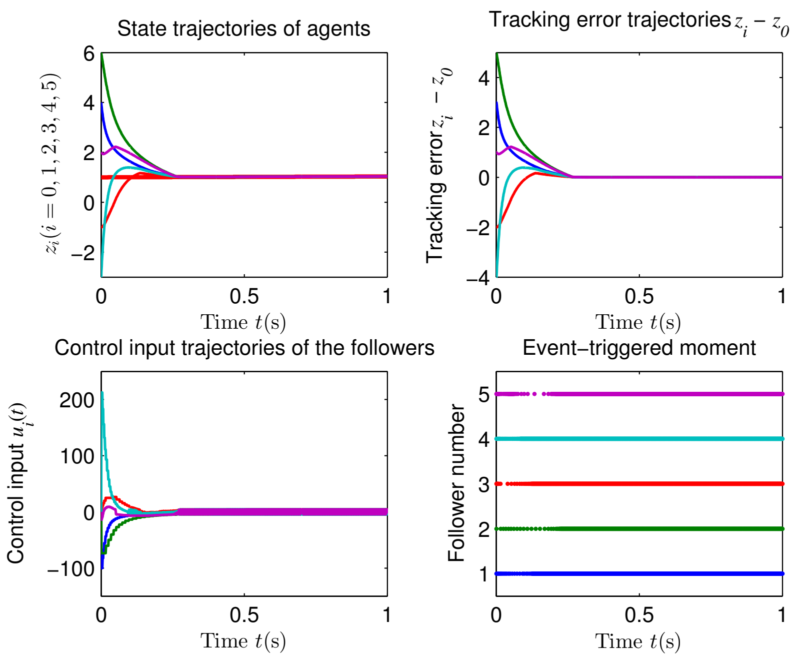

Figure 13. Simulation results with the controller in [25] under $\mathcal{G}_1$.

Example 2. Simulation on a multiple UAV system: Consider a MAS consisting of five UAVs with a multi-layer control structure applied in [32]. The inner-loop controller provides sufficient effectiveness to achieve accurate and rapid tracking of reference signals. Consequently, the control design can focus on the outer loop, which governs the UAV positions. The outer-loop dynamics of the ith UAV can be approximated by $\dot{z}_i(t) = u_i(t)$, where $z_i(t) \in \mathcal{R}^3$ represents the position and $u_i(t) \in \mathcal{R}^3$ represents the control input [32].

It is assumed that time delays exist in the information exchange among different UAVs, and the follower UAVs are affected by external disturbances, with the leader UAV denoted by 0 and the remaining follower UAVs denoted by 1, 2, 3, 4. Their dynamics are modeled as follows.

$$\dot{z}_0(t) = 0.1z_0(t) + 0.1 \times \begin{pmatrix} 0.8 - 2.3\sin(0.1\pi t) + 1.8\cos(0.1\pi t) \\ 0.8 + 2.2\sin(0.1\pi t) + 1.9\cos(0.1\pi t) \\ 1.7 - 1.8\cos(0.1\pi t) \end{pmatrix}$$

$$\begin{aligned} \dot{z}_i(t) = 0.1z_i(t) + 0.1 \times &\begin{pmatrix} 0.8 - 2.3\sin(0.1\pi t) + 1.8\cos(0.1\pi t) \\ 0.8 + 2.2\sin(0.1\pi t) + 1.9\cos(0.1\pi t) \\ 1.7 - 1.8\cos(0.1\pi t) \end{pmatrix} \\ &+ u_i(t, z_i(t), z_i(t-\tau)) + 0.12\sin\left(3t + \frac{\pi}{5}\right)\begin{pmatrix} 1.5 \\ 0.5 \\ -2 \end{pmatrix}, \quad i = 1, 2, 3, 4. \end{aligned}$$

In simulation, the switching topologies are shown in Figure 14. From the above dynamics model, it can be easily confirmed that the nonlinear function fulfills Assumption 2, where the constant l is taken as 0.1 and the external disturbance fulfills Assumption 3 with the constant $d = 0.36$. Suppose that the information of the initial state for each agent is selected as $z_0(0) = (1, 0.5, -1)^{\mathrm{T}}, z_1(0) = (4, 1, -2)^{\mathrm{T}}, z_2(0) = (6, 2, 0)^{\mathrm{T}}, z_3(0) = (-1, 3, 1)^{\mathrm{T}}, z_4(0) = (-3, 0, 2)^{\mathrm{T}}$. To achieve the control objective, the control gains are set as $\kappa_1 = 0.1, \kappa_2 = 5.48, \kappa_3 = 1.05, \bar{d} = 5.2$, and the other parameters are set as $q = 2.52, \tau = 0.05, \rho_i = 0.75, i = 1, 2, 3, 4$. Thus far, by some simple calculations, it can be verified that the conditions in Theorem 3 hold. Therefore, FxTC tracking is reached. Furthermore, the ST upper bound can be evaluated as $\mathcal{T}^3_{max} = 3.3519$ s.

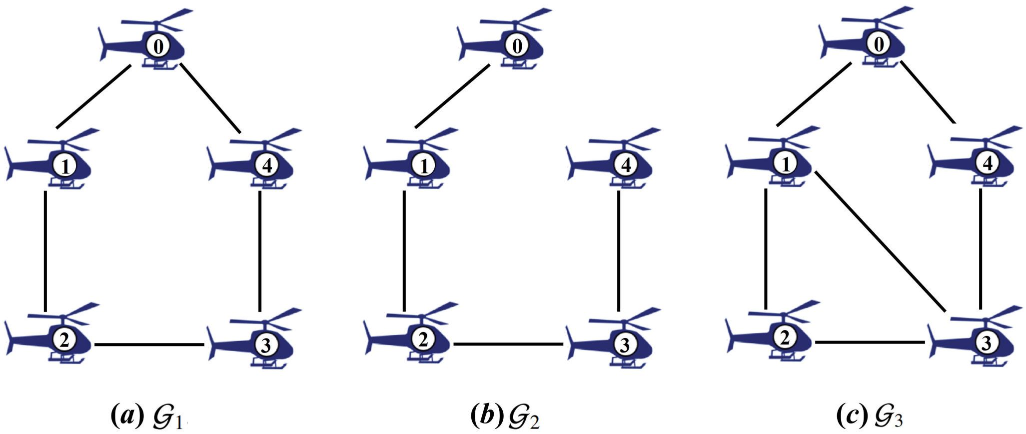

Figure 14. Switching topologies of leader-following UAVs.

The simulation results are displayed in Figures 15–17. Figure 15 displays the leader and follower UAV's state trajectories. It is easy to observe that the four follower UAVs achieve FxTC tracking within 0.3 s, and the actual ST meets the requirement of the ST upper bound $\mathcal{T}^3_{max}$. Figure 16 shows every follower UAV's tracking error trajectory $z_i(t) - z_0(t)$. Figure 17 depicts the inter-event intervals of the follower UAVs. In conclusion, under the proposed controller, the considered multi-UAV system achieves FxTC tracking within the upper bound of ST $\mathcal{T}^3_{max}$.

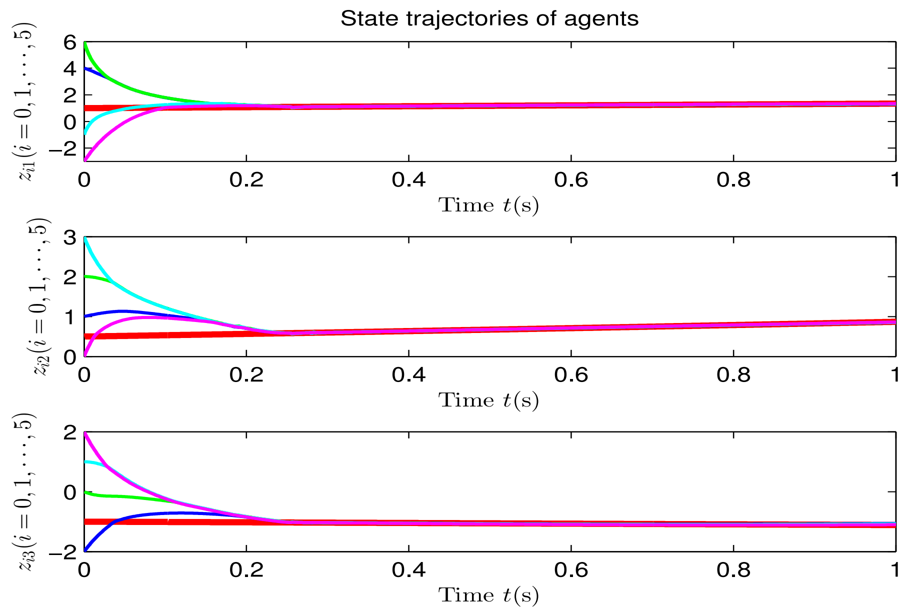

Figure 15. State trajectories of a multi-UAV system under switching topologies.

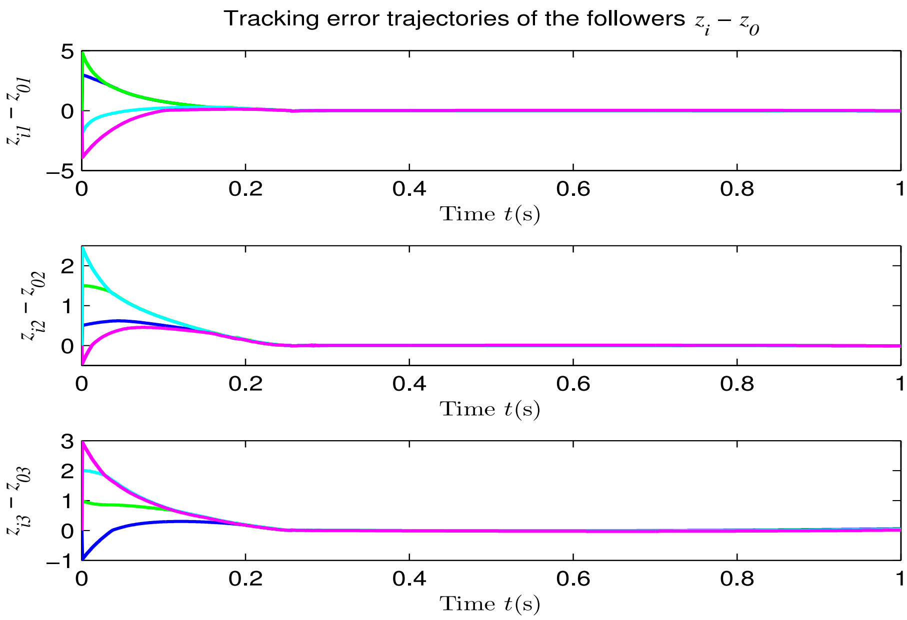

Figure 16. Tracking error trajectories of a multi-UAV system under switching topologies.

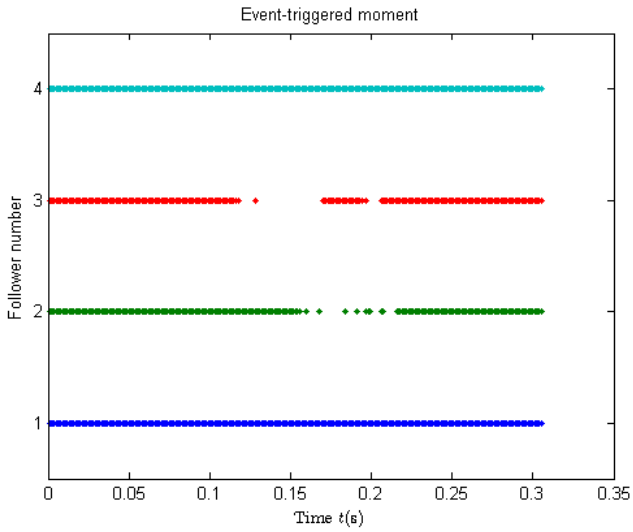

Figure 17. Triggering instants of followers under switching topologies.

5. Conclusions

The problem of FxTC tracking is investigated for nonlinear delayed MASs with external disturbances under switching topologies. A novel nonlinear and discontinuous ET controller, incorporating time delays, is designed. After that, FxTC theorems are established for both fixed and switching topologies. Simultaneously, the estimated ST upper bounds are directly computed by using the system's predetermined parameters. What is more, Zeno behavior is avoided. Simulation examples are provided to demonstrate the validity and advantage of the theoretical findings. Future work will focus on extending the proposed method to second-order and higher-order nonlinear delayed MASs. Furthermore, the influence of time delay on systems, the issues of sensor and actuator faults on MASs, and physical validation will also be future research directions.

Author contributions

Mingqiang Meng: Methodology, formal analysis, writing–original draft and software; Kaiquan Xiang: Software and validation; Qintao Gan: Formal analysis, writing–review and editing; Lei Chang: Validation, writing–review and editing. All authors have read and approved the final version of the manuscript for publication.

Use of AI tools declaration

The authors declare that they have not used Artificial Intelligence (AI) tools in the creation of this article.

Acknowledgments

The authors are grateful to the editor and reviewers for their insightful comments and suggestions, which greatly improved this article. This work was supported by the National Natural Science Foundation of China under Grant No.61305076.

Conflict of interest

All authors declare no conflicts of interest in this paper.

References

1. F. L. Sun, J. S. Su, W. Zhu, Z. H. Guan, J. Kurths, Predefined-time formation control of UAV swarm under spatiotemporal constraints, *ISA T.*, **170** (2026), 187–199. https://doi.org/10.1016/j.isatra.2026.01.025
2. T. S. Chu, J. Wang, L. Codeca, Z. J. Li, Multi-agent deep reinforcement learning for large-scale traffic signal control, *IEEE T. Intell. Transp.*, **21** (2020), 1086–1095. http://doi.org/10.1109/TITS.2019.2901791
3. J. Huang, T. T. Zhao, W. J. Lu, J. Z. Zeng, Y. T. Chen, Practical fixed-time formation control for wheeled robots: An approach based on time-base generators, *Int. J. Robust Nonlin.*, **36** (2026), 816–829. https://doi.org/10.1002/rnc.70172
4. D. Yue, C. Deng, C. Y. Wen, W. Wang, Finite-time distributed resilient tracking control for nonlinear MASs with application to power systems, *IEEE T. Automat. Contr.*, **69** (2024), 3128–3143. http://doi.org/10.1109/TAC.2023.3332777
5. Y. P. Luo, X. T. Gao, A. P. Li, A. Kashkynbayev, Event-triggered finite-time formation control for second-order leader-following multi-agent systems with nonlinear term time delay, *Int. J. Control*, **96** (2023), 2636–2650. http://doi.org/10.1080/00207179.2022.2106898
6. X. Wang, S. D. Wang, J. Liu, Y. B. Wu, C. Y. Sun, Bipartite finite-time consensus of multi-agent systems with intermittent communication via event-triggered impulsive control, *Neurocomputing*, **598** (2024), 127970. https://doi.org/10.1016/j.neucom.2024.127970
7. X. Wang, W. W. Guang, T. W. Huang, J. Kurths, Optimized adaptive finite-time consensus control for stochastic nonlinear multiagent systems with non-affine nonlinear faults, *IEEE T. Autom. Sci. Eng.*, **21** (2024), 5012–5023. https://doi.org/10.1109/TASE.2023.3306101
8. B. Ning, J. Jin, J. C. Zheng, Z. H. Man, Finite-time and fixed-time leader-following consensus for multi-agent systems with discontinuous inherent dynamics, *Int. J. Control*, **91** (2018), 1259–1270. http://doi.org/10.1080/00207179.2017.1313453
9. M. L. Liu, Y. N. Guo, G. T. Ran, J. H. Park, Fixed-time consensus tracking control for nonlinear multi-agent systems: A dynamic edge/self-triggered approach, *IEEE T. Circuits-II*, **73** (2026), 73–77. http://doi.org/10.1109/TCSII.2025.3637122
10. J. K. Ni, Y. Tang, P. Shi, A new fixed-time consensus tracking approach for second-order multiagent systems under directed communication topology, *IEEE T. Syst. Man Cy.*, **51** (2021), 2488–2500. http://doi.org/10.1109/TSMC.2019.2915562

11. Q. Jia, Z. Y. Han, W. K. S. Tang, Synchronization of multi-agent systems with time-varying control and delayed communications, *IEEE T. Circuits-I*, **66** (2019), 4429–4438. http://doi.org/10.1109/TCSI.2019.2928040

12. J. Zhang, G. P. Liu, Model-free distributed integral sliding mode predictive control for multi-agent systems with communication delay, *Neurocomputing*, **569** (2024), 127133. https://doi.org/10.1016/j.neucom.2023.127133

13. L. L. Zhang, S. S. Liu, C. C. Hua, Leader-following consensus control for nonlinear multiagent systems with unknown time-varying measurement sensitivity and infinite communication delays, *J. Frankl. I.*, **361** (2024), 1127–1139. https://doi.org/10.1016/j.jfranklin.2023.12.059

14. J. K. Ni, Y. Zhao, J. D. Cao, W. L. Li, Fixed-time practical consensus tracking of multi-agent systems with communication delay, *IEEE T. Netw. Sci. Eng.*, **9** (2022), 1319–1334. http://doi.org/10.1109/TNSE.2022.3140592

15. J. Liu, Y. L. Zhang, C. Y. Sun, Y. Yu, Fixed-time consensus of multi-agent systems with input delay and uncertain disturbances via event-triggered control, *Inform. Sciences*, **480** (2019), 261–272. https://doi.org/10.1016/j.ins.2018.12.037

16. M. Q. Meng, Q. T. Gan, R. H. Li, L. K. Li, Q. K. Kang, H. Chang, Improved fixed-time consensus of delayed nonlinear leader–follower multi-agent systems: A new stability approach, *Nonlinear Anal.-Model.*, **31** (2026), 398–420. https://doi.org/10.15388/namc.2026.31.45328

17. R. X. Lu, J. Wu, X. S. Zhan, H. C. Yan, Practical fixed-time event-triggered output feedback containment control for second-order nonlinear multi-agent systems with switching topologies, *Neurocomputing*, **585** (2024), 127580. https://doi.org/10.1016/j.neucom.2024.127580

18. J. Liu, Y. Yu, Y. Xu, Y. L. Zhang, C. Y. Sun, Fixed-Time average consensus of nonlinear delayed MASs under switching topologies: An event-based triggering approach, *IEEE T. Syst. Man Cy.*, **52** (2022), 2721–2733. http://doi.org/10.1109/TSMC.2021.3051156

19. H. Y. Yang, Y. J. Wang, Finite-gain based prescribed-time consensus control for multi-agent systems under switching topology, *Automatica*, **183** (2026), 112686. https://doi.org/10.1016/j.automatica.2025.112686

20. H. Wang, W. W. Yu, G. H. Wen, G. R. Chen, Fixed-time consensus of nonlinear multi-agent systems with general directed topologies, *IEEE T. Circuits-II*, **66** (2019), 1587–1591. http://doi.org/10.1109/TCSII.2018.2886298

21. X. W. Li, Y. Tang, H. R. Karimi, Consensus of multi-agent systems via fully distributed event-triggered control, *Automatica*, **116** (2020), 108898. https://doi.org/10.1016/j.automatica.2020.108898

22. H. J. Liu, Z. Y. Yu, H. J. Jiang, Fixed-time consensus of nonlinear multi-agent systems via both event-triggered intermittent communication and sampled-data control, *Commun. Nonlinear Sci.*, **140** (2025), 108391. https://doi.org/10.1016/j.cnsns.2024.108391

23. X. Wang, N. Pang, Y. W. Xu, T. W. Huang, J. Kurths, On state-constrained containment control for nonlinear multiagent systems using event-triggered input, *IEEE T. Syst. Man Cy.*, **54** (2024), 2530–2538. https://doi.org/10.1109/TSMC.2023.3345365

24. H. Mei, X. Wen, Predefined-time output feedback consensus control for leader–follower second-order multiagent systems with actuator faults and input saturation based on event-triggered mechanism, *Int. J. Dynam. Control*, **13** (2025), 74. https://doi.org/10.1007/s40435-024-01514-4

25. W. Zhang, Q. Huang, A. Alhudhaif, Event-triggered fixed-time bipartite consensus for nonlinear disturbed multi-agent systems with leader-follower and leaderless controller, *Inform. Sciences*, **662** (2024), 120243. https://doi.org/10.1016/j.ins.2024.120243

26. S. C. Zhang, D. C. Liu, Y. W. Zhang, C. R. Chen, Event-triggered predefined-time sliding mode control for consensus of nonlinear multi-agent systems with disturbances, *Commun. Nonlinear Sci.*, **152** (2026), 109331. https://doi.org/10.1016/j.cnsns.2025.109331

27. X. Y. Liu, L. X. Wang, J. D. Cao, Further results on fixed-time leader-following consensus of heterogeneous multiagent systems with external disturbances, *IEEE T. Syst. Man Cy.*, **54** (2024), 416–425. http://doi.org/10.1109/TSMC.2023.3309867

28. S. X. Sun, X. Dai, X. X. Hua, J. Duan, Y. L. Li, F. D. Yu, Observer-based fixed-time consensus control for nonlinear multiagent systems, *Int. J. Control Autom. Syst.*, **22** (2024), 2812–2822. http://doi.org/10.1007/s12555-023-0903-8

29. L. Wang, F. Xiao, Finite-time consensus problems for networks of dynamic agents, *IEEE T. Automat. Contr.*, **55** (2010), 950–955. http://doi.org/10.1109/TAC.2010.2041610

30. F. C. Jiang, L. Wang, Finite-time information consensus for multi-agent systems with fixed and switching topologies, *Physica D*, **238** (2009), 1550–1560. https://doi.org/10.1016/j.physd.2009.04.011

31. X. L. Ai, L. Wang, Distributed fixed-time event-triggered consensus of linear multi-agent systems with input delay, *Int. J. Robust Nonlin.*, **31** (2021), 2526–2545. https://doi.org/10.1002/rnc.5404

32. J. Su, Y. D. Song, Prescribed-time formation control for multi-agent systems with uncertain nonlinear dynamics and non-vanishing random disturbances, *IEEE-CAA J. Automatic.*, **13** (2026), 586–596. http://doi.org/10.1109/JAS.2026.125714

AIMS Press